

## **Electronic Supplementary Information for**

# **Zn(II) complexes with thiazolyl-hydrazone: structure, intermolecular interactions, photophysical properties, computational study and anticancer activity**

Jovana B. Araškov<sup>a</sup>, Aleksandar Višnjevac<sup>b</sup>, Jasmina Popović<sup>b</sup>, Vladimir Blagojević<sup>c</sup>,  
Henrique S. Fernandes<sup>d,e</sup>, Sérgio F. Sousa<sup>d,e</sup>, Irena Novaković<sup>f</sup>, José M. Padrón<sup>g</sup>,  
Berta Barta Holló<sup>h</sup>, Miguel Monge<sup>i</sup>, María Rodríguez-Castillo<sup>i</sup>,  
José M. López-de-Luzuriaga<sup>i\*</sup>, Nenad R. Filipović<sup>j</sup>, Tamara R. Todorović<sup>a\*</sup>

<sup>a</sup>*University of Belgrade - Faculty of Chemistry, Studentski trg 12-16, 11000 Belgrade, Serbia;* <sup>b</sup>*Division of Physical Chemistry, Institute Ruđer Bošković, Bijenička cesta 54, 10000 Zagreb, Croatia;* <sup>c</sup>*Institute of Technical Sciences of the Serbian Academy of Sciences and Arts, Knez Mihailova 35/IV, 11000 Belgrade, Serbia;* <sup>d</sup>*UCIBIO – Applied Molecular Biosciences Unit, BioSIM – Department of Biomedicine, Faculty of Medicine, University of Porto, 4200-319 Porto, Portugal;* <sup>e</sup>*Associate Laboratory i4HB – Institute for Health and Bioeconomy, Faculty of Medicine, University of Porto, 4200-319 Porto, Portugal;* <sup>f</sup>*Institute of Chemistry, Technology and Metallurgy, University of Belgrade, Njegoševa 12, 11000, Belgrade, Serbia;* <sup>g</sup>*BioLab, Instituto Universitario de Bio-Orgánica “Antonio González”, Universidad de La Laguna, 38071 La Laguna, Spain;* <sup>h</sup>*University of Novi Sad, Faculty of Sciences, Trg Dositeja Obradovića 4, 21000 Novi Sad, Serbia;* <sup>i</sup>*Departamento de Química, Universidad de La Rioja, Centro de Investigación en Síntesis Química (CISQ), Complejo Científico-Tecnológico, 26004-Logroño, Spain;* <sup>j</sup>*University of Belgrade - Faculty of Agriculture, Nemanjina 6, 11000 Belgrade, Serbia*

\*Corresponding Authors:

Tamara R. Todorović, University of Belgrade - Faculty of Chemistry, Studentski trg 12-16, 11000 Belgrade, Serbia E-mail: [tamarat@chem.bg.ac.rs](mailto:tamarat@chem.bg.ac.rs)

José M. López-de-Luzuriaga, Departamento de Química, Universidad de La Rioja, Centro de Investigación en Síntesis Química (CISQ), Complejo Científico-Tecnológico, 26004-Logroño, Spain; E-mail: [josemaria.lopez@unirioja.es](mailto:josemaria.lopez@unirioja.es)

## Contents

1. IR and NMR spectroscopy .....	3
2. Crystallography .....	14
3. Hirshfeld analysis.....	23
4. Intermolecular interaction energies and energy frameworks .....	26
5. Thermal stability .....	37
6. Photoluminescence and DFT and TD-DFT computational study .....	37

## 1. IR and NMR spectroscopy

IR spectra were recorded on a Thermo Scientific Nicolet 6700 FT-IR spectrometer by the Attenuated Total Reflection (ATR) technique in the region 4000–400 cm<sup>-1</sup>.

The NMR spectra were performed on a Bruker Avance 500 and Varian / Agilent 400 equipped with the broad-band direct probe. NMR spectra were recorded in DMSO-*d*<sub>6</sub> and chemical shifts are given on  $\delta$  scale relative to TMS (0.03 % v/v) as an internal standard for <sup>1</sup>H and <sup>13</sup>C.

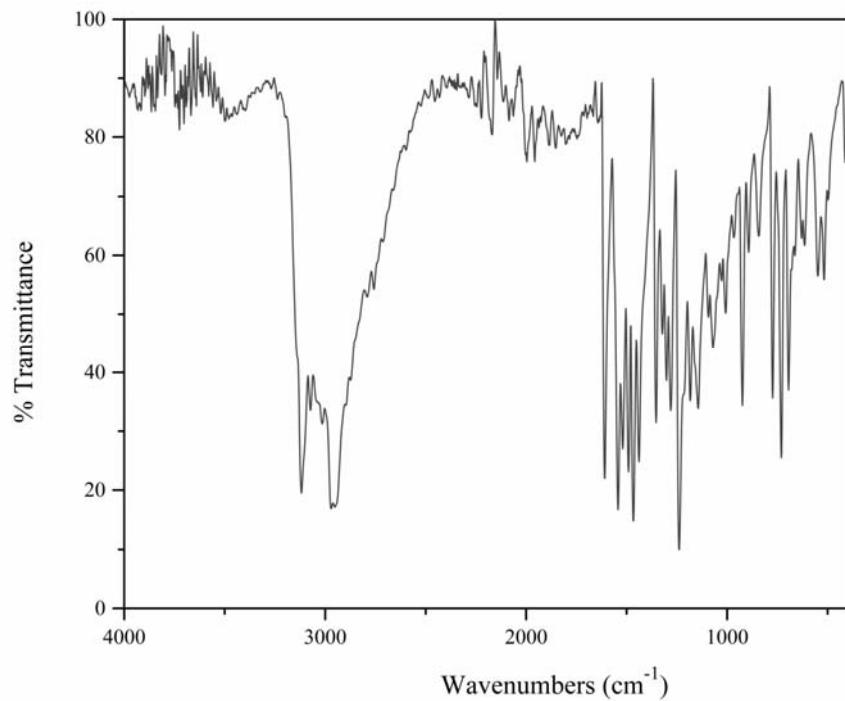


Figure S1. IR spectrum of **1-Cl**

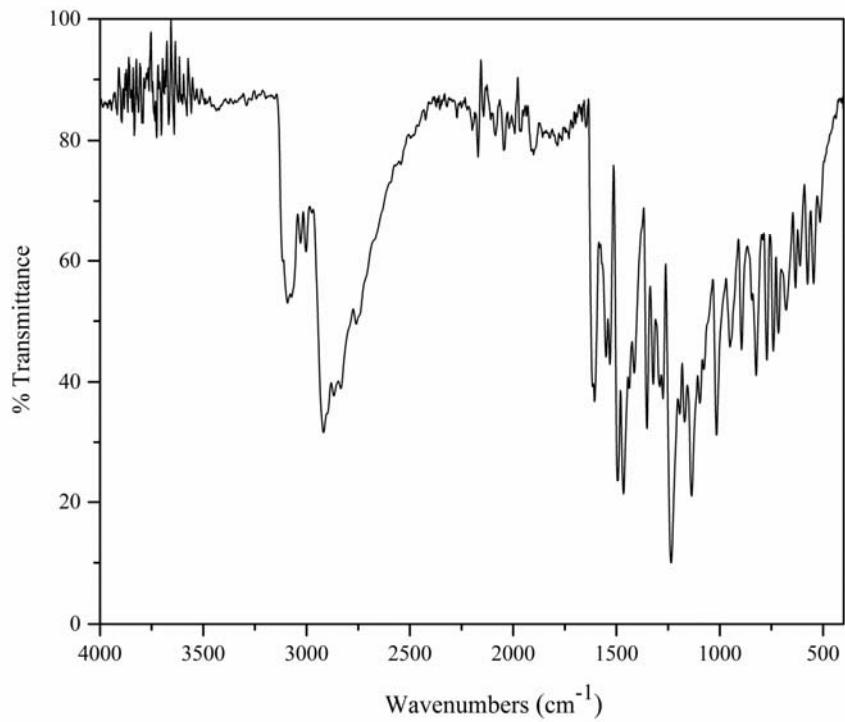


Figure S2. IR spectrum of **2-Cl**

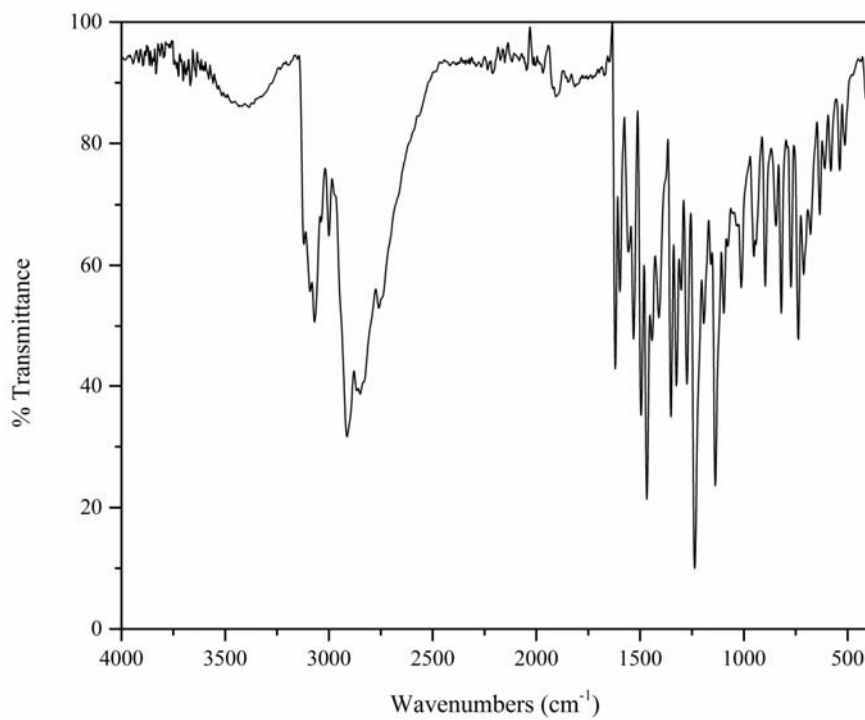


Figure S3. IR spectrum of **3-Cl**

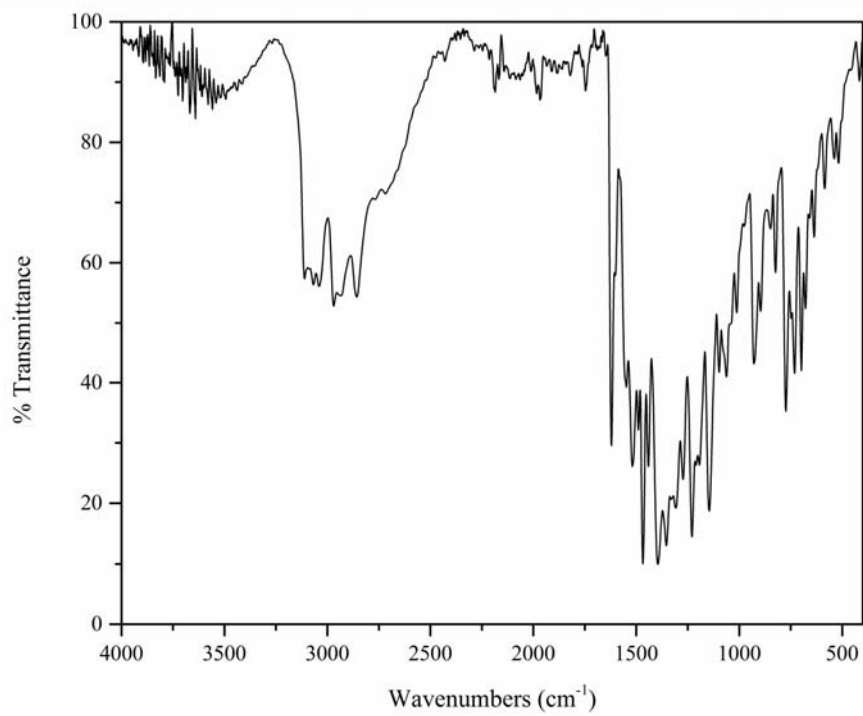


Figure S4. IR spectrum of **1-NO<sub>3</sub>**

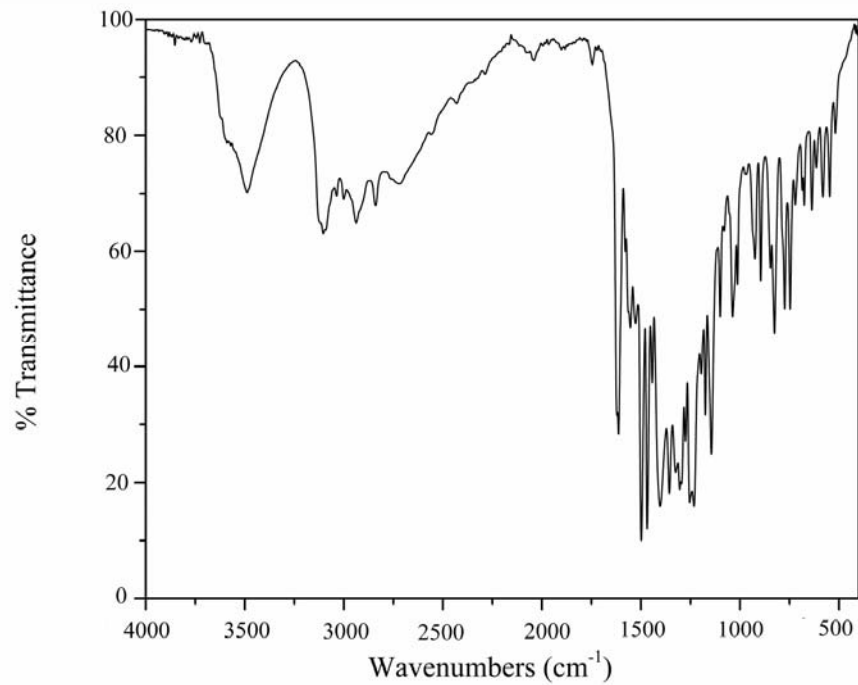


Figure S5. IR spectrum of **2-NO<sub>3</sub>**.

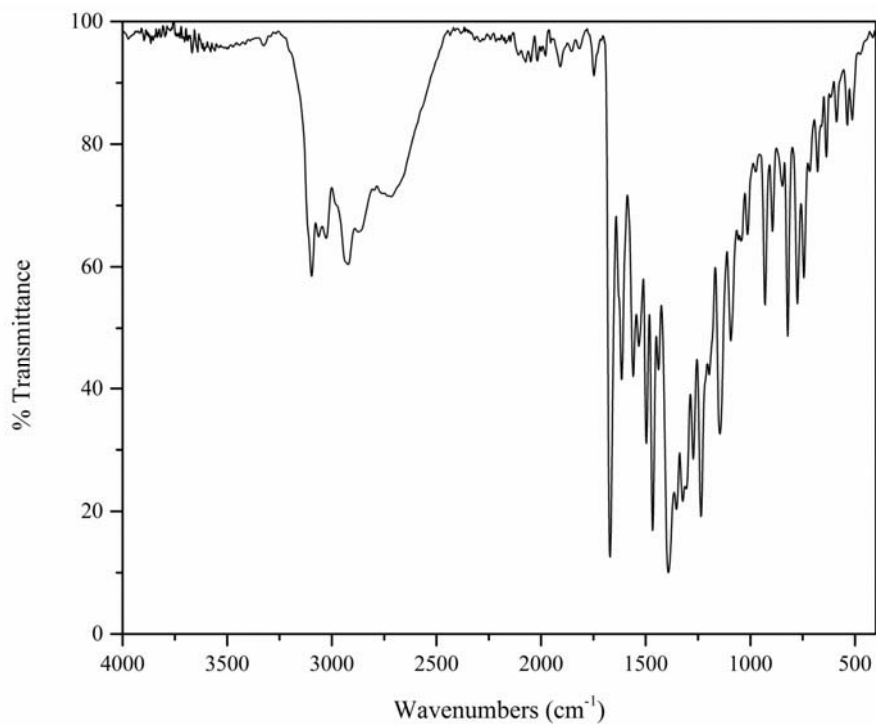


Figure S6. IR spectrum of **3-NO<sub>3</sub>**.

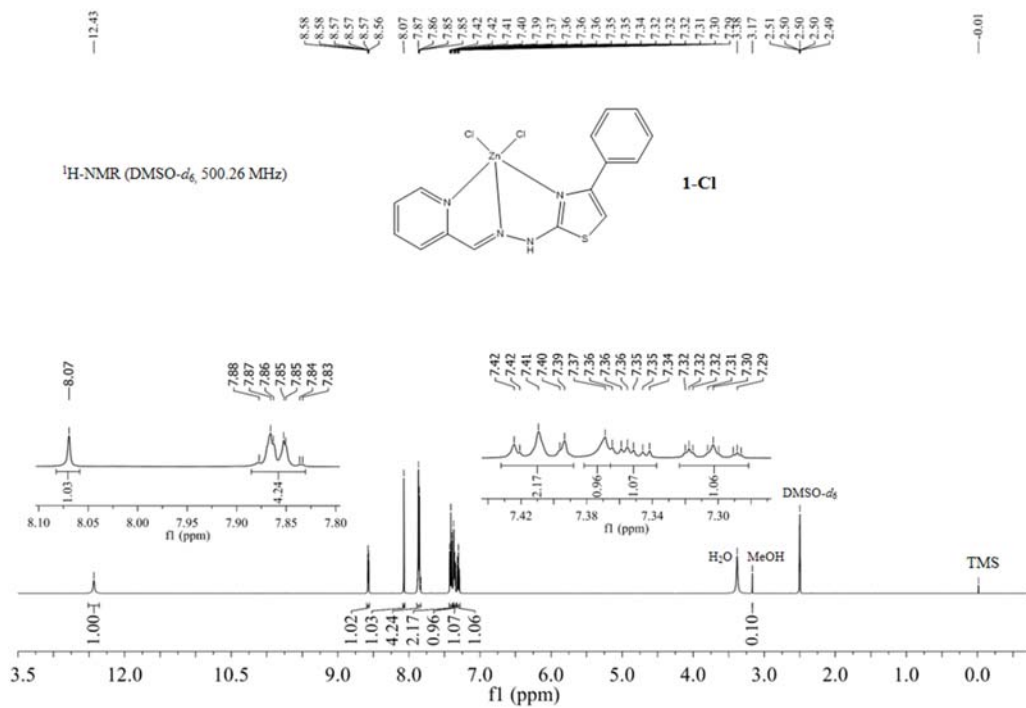


Figure S7. <sup>1</sup>H-NMR spectrum of **1-Cl** in DMSO-*d*<sub>6</sub>.

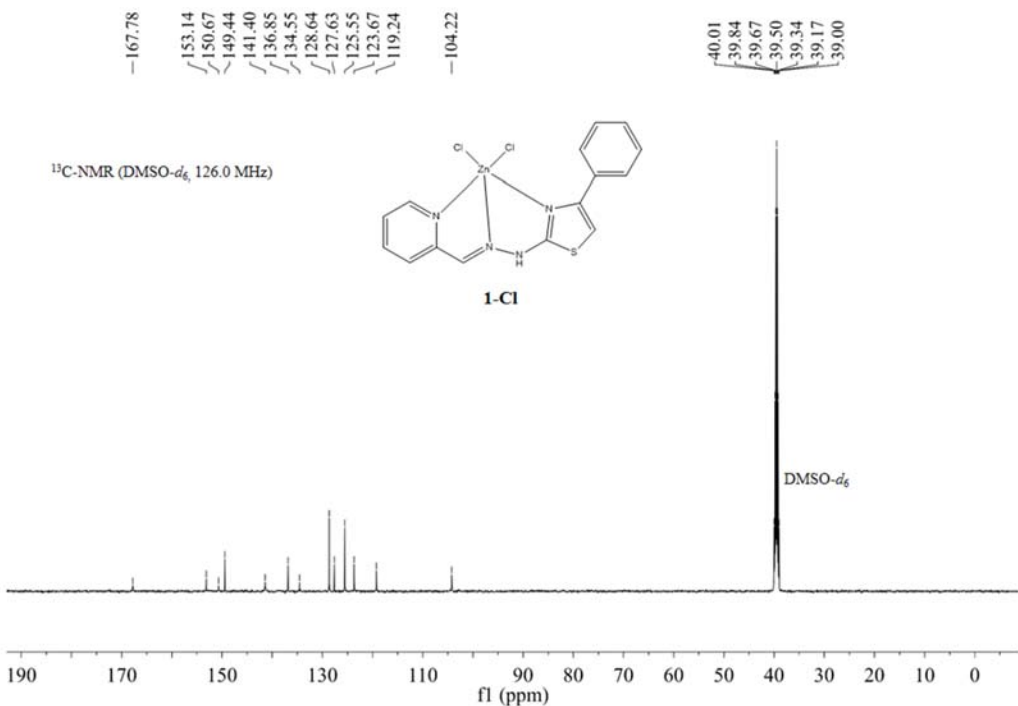


Figure S8. <sup>13</sup>C NMR spectrum of **1-Cl** in DMSO-*d*<sub>6</sub>.

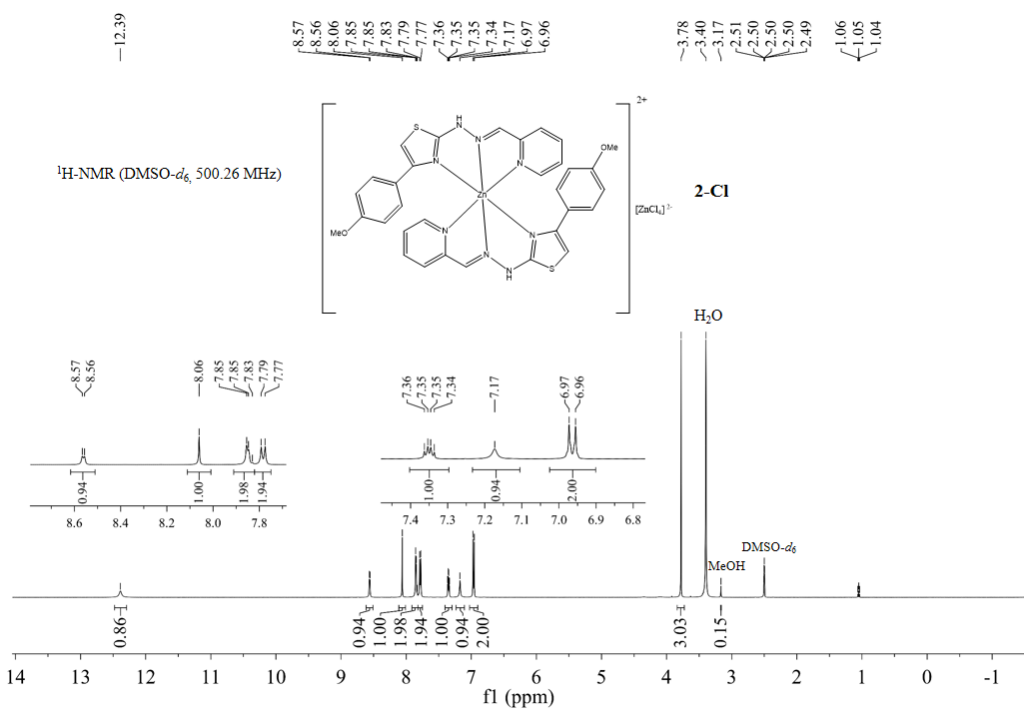


Figure S9. <sup>1</sup>H NMR spectrum of **2-Cl** in DMSO-*d*<sub>6</sub>.

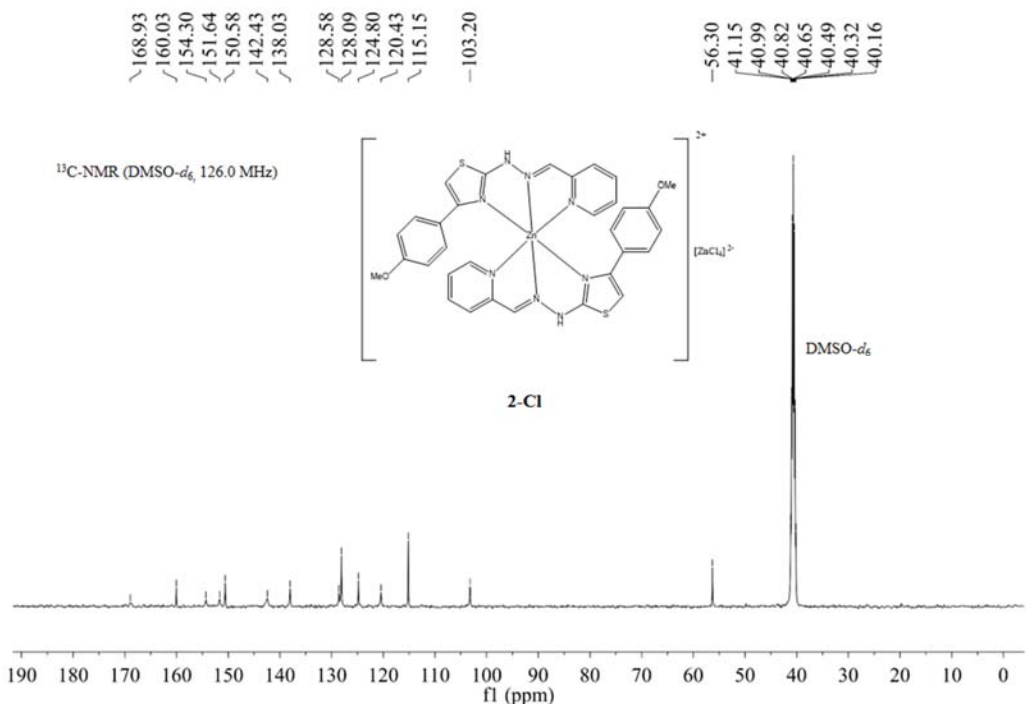


Figure S10.  $^{13}\text{C}$  NMR spectrum of **2-Cl** in  $\text{DMSO}-d_6$ .

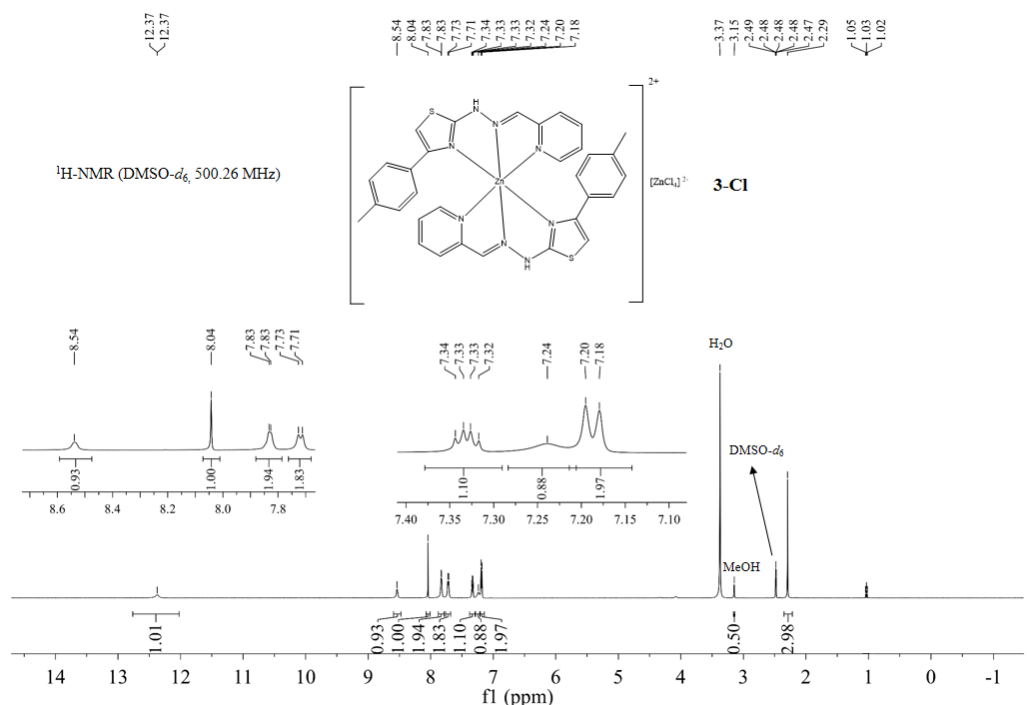


Figure S11.  $^1\text{H}$  NMR spectrum of **3-Cl** in  $\text{DMSO}-d_6$ .

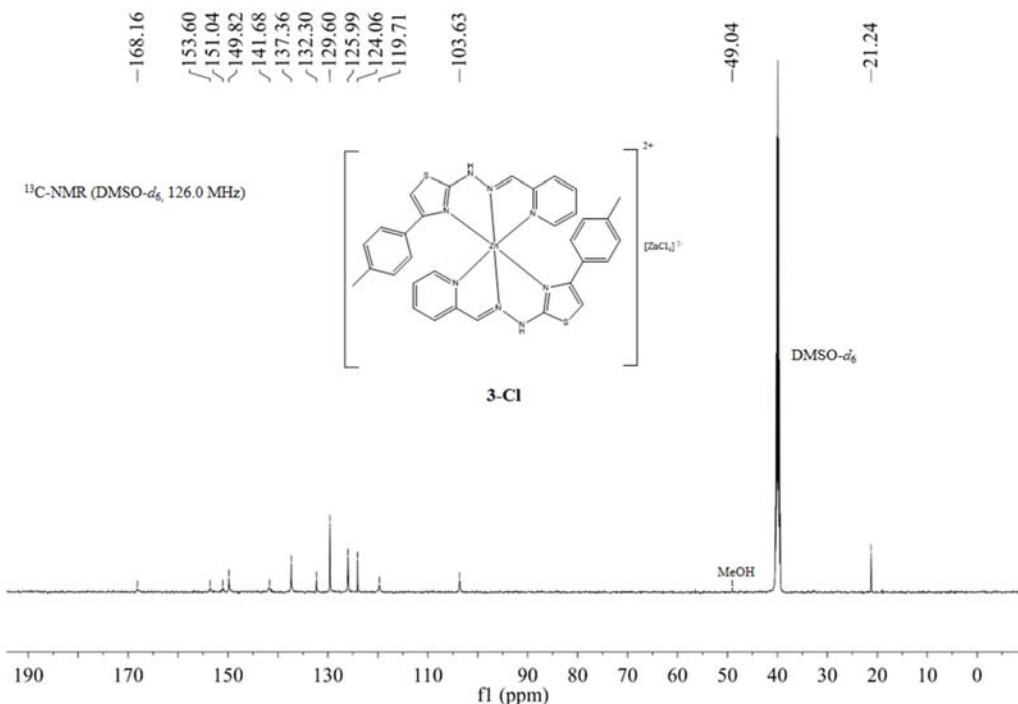


Figure S12. <sup>13</sup>C NMR spectrum of **3-Cl** in DMSO-*d*<sub>6</sub>.

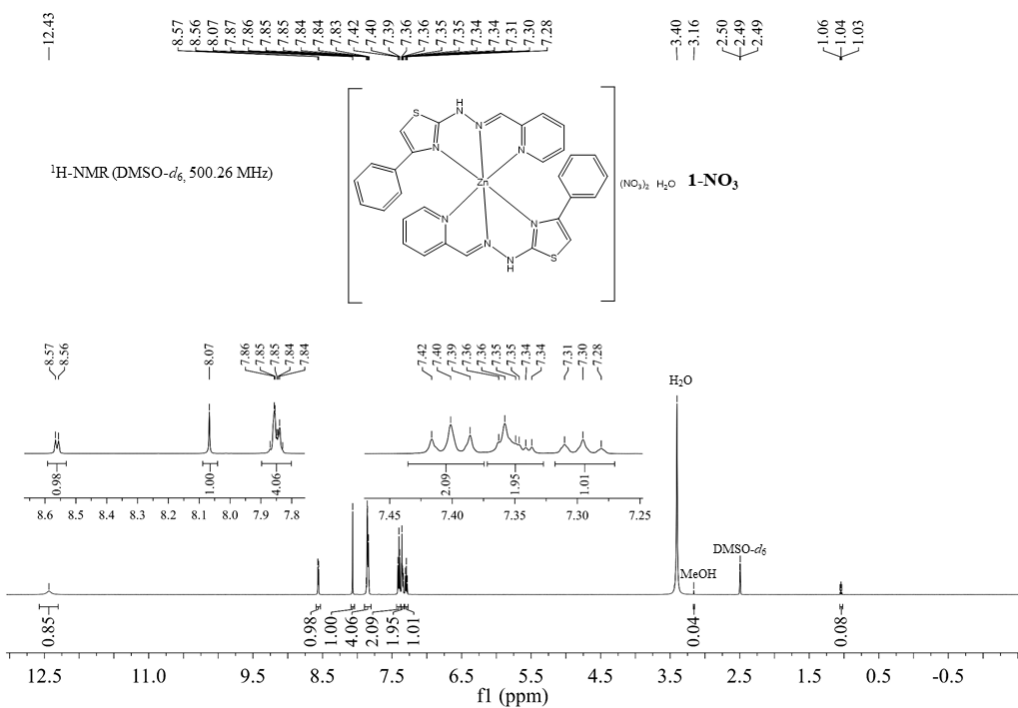


Figure S13. <sup>1</sup>H NMR spectrum of **1-NO**<sub>3</sub> in DMSO-*d*<sub>6</sub>.

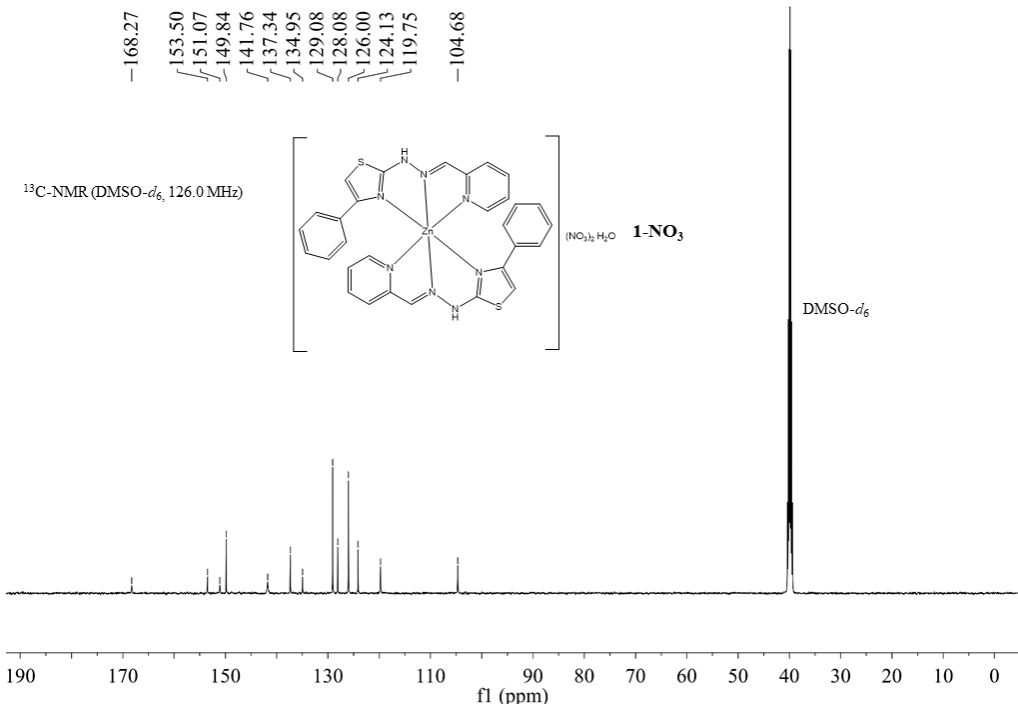


Figure S14. <sup>13</sup>C NMR spectrum of **1-NO<sub>3</sub>** in DMSO-*d*<sub>6</sub>.

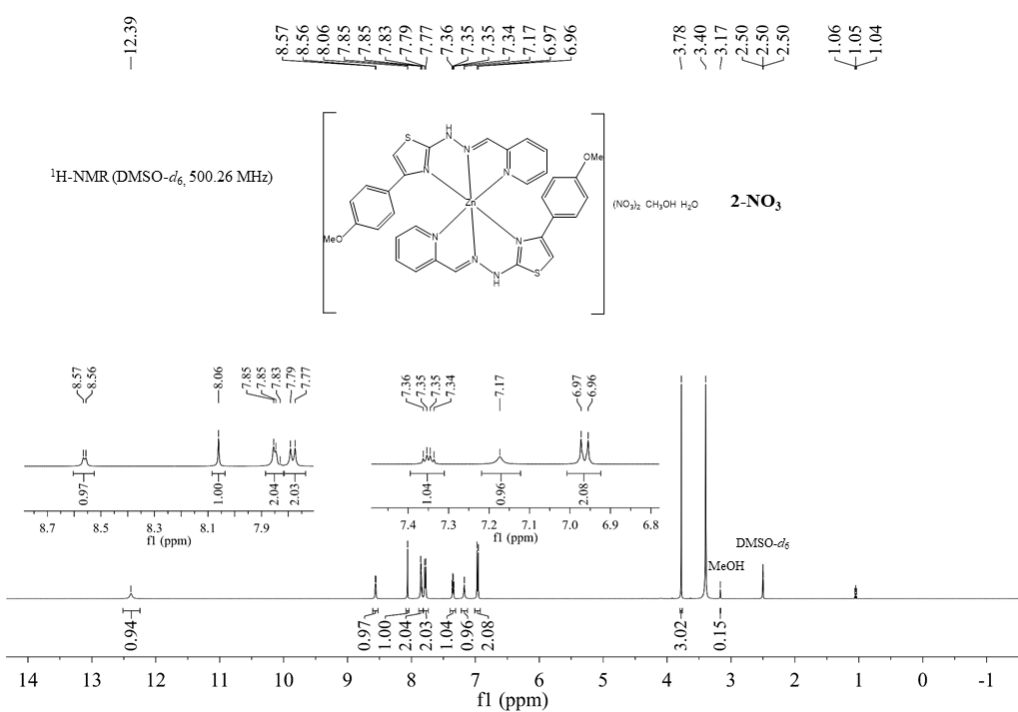


Figure S15. <sup>1</sup>H NMR spectrum of **2-NO<sub>3</sub>** in DMSO-*d*<sub>6</sub>.

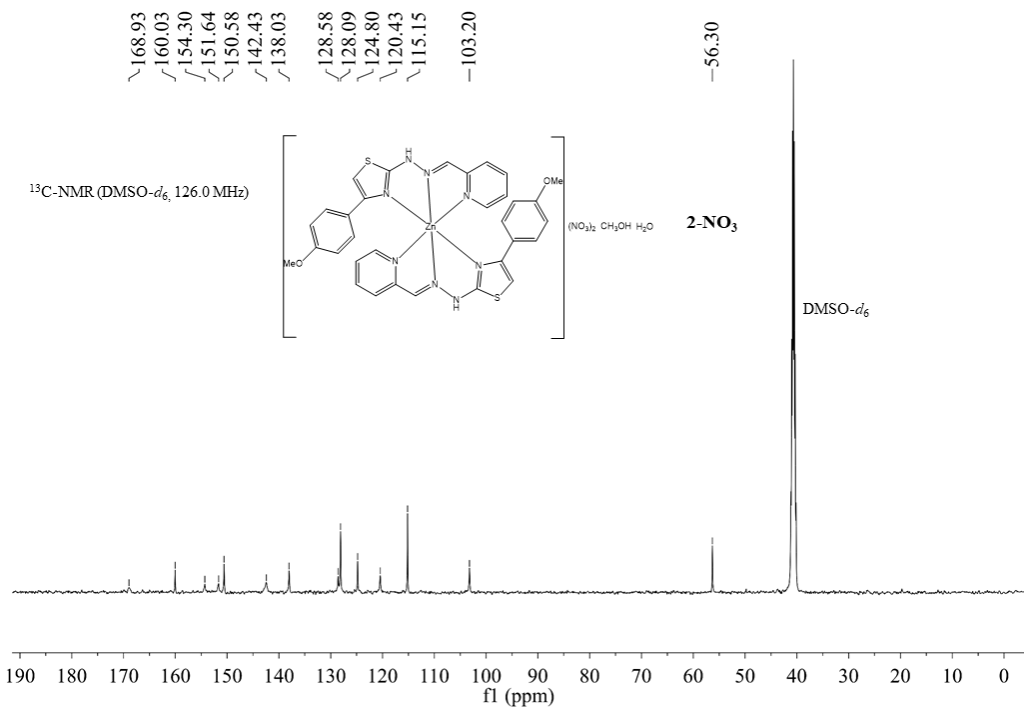


Figure S16.  $^{13}\text{C}$  NMR spectrum of **2-NO<sub>3</sub>** in DMSO-*d*<sub>6</sub>.

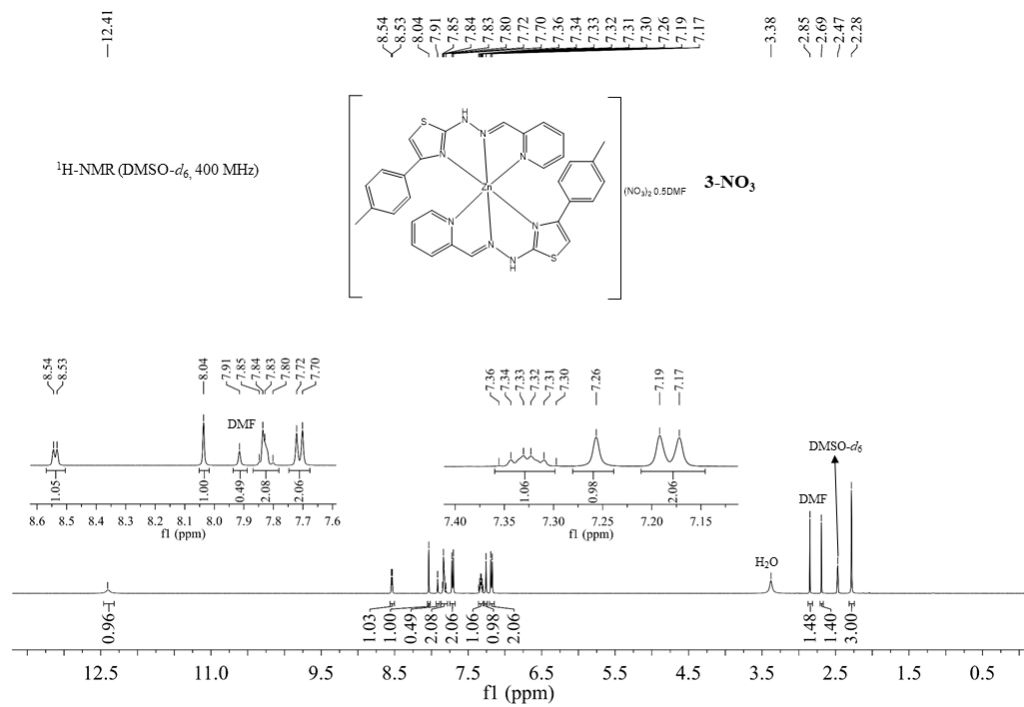


Figure S17.  $^1\text{H}$  NMR spectrum of **3-NO<sub>2</sub>** in DMSO-*d*<sub>6</sub>.

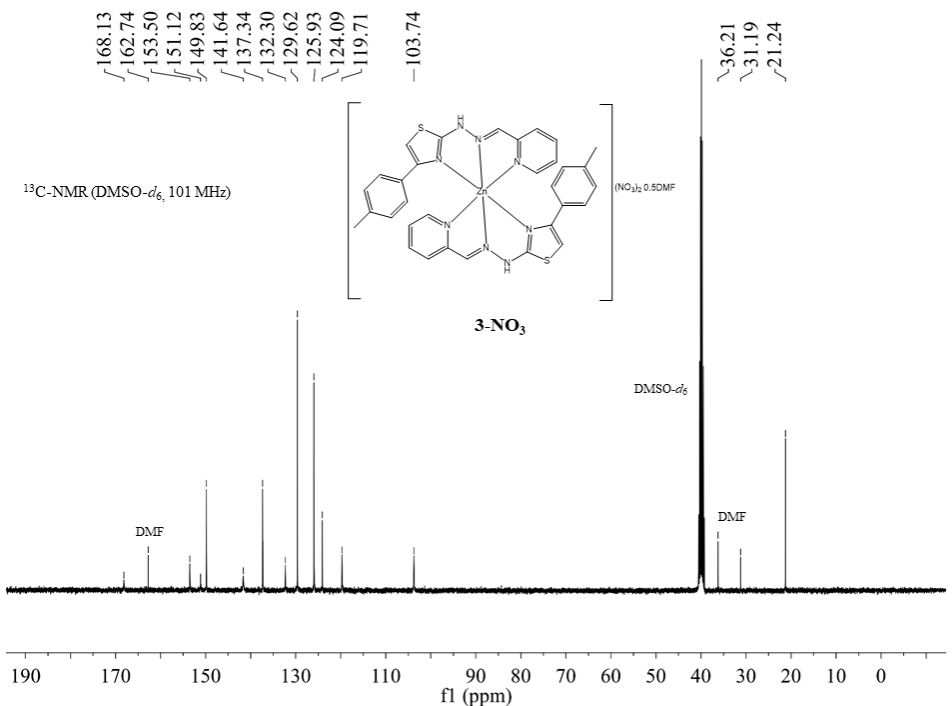


Figure S18. <sup>13</sup>C NMR spectrum of **3-NO<sub>3</sub>** in DMSO-*d*<sub>6</sub>.

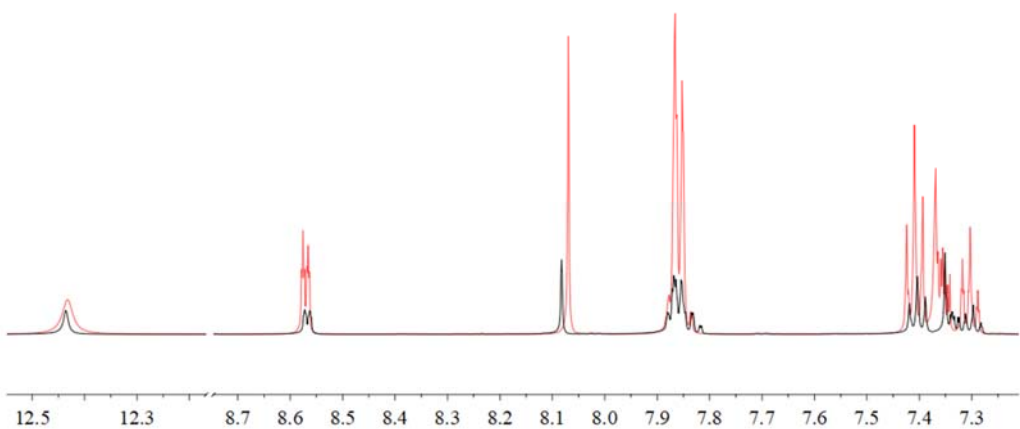


Figure S19. Overlay of <sup>1</sup>H NMR spectra of **1-Cl** (red) and **HLS<sup>1</sup>** (black).

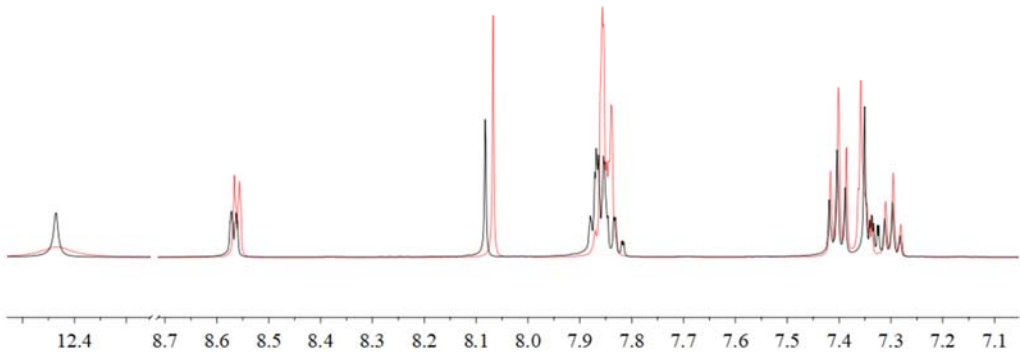


Figure S20. Overlay of <sup>1</sup>H NMR spectra of **1-NO<sub>3</sub>** (red) and **HLS<sup>1</sup>** (black).

## 2. Crystallography

Table S1. Bond angles ( $^{\circ}$ ) within the coordination sphere of **1–3-Cl** and **1–3-NO<sub>3</sub>**

Angles ( $^{\circ}$ )	<b>1-NO<sub>3</sub></b>	<b>2-NO<sub>3</sub></b>	<b>3-NO<sub>3</sub></b>	Angles ( $^{\circ}$ )	<b>1-Cl</b>	Angles ( $^{\circ}$ )	<b>2-Cl</b>	<b>3-Cl</b>
N1–Zn–N2	73.63(13)	73.42(13)	73.31 (7)	N1–Zn1–N2	72.29(9)	N1–Zn1–N2	73.29(9)	73.12 (14)
N1–Zn1–N4	148.52 (12)	146.62(13)	147.50 (8)	N1–Zn1–N4	145.95(9)	N1–Zn1–N4	146.79(9)	146.39(17)
N1–Zn1–N5	89.41(11)	87.67(13)	89.78 (7)	N2–Zn1–N4	73.71(8)	N1–Zn1–N1i*	88.33(8)	90.51(14)
N–Zn1–N6	92.04(11)	93.73(13)	93.79 (7)	Cl1–Zn1–Cl2	119.45(3)	N1–Zn1–N2i	93.28(9)	93.06(15)
N1–Zn1–N8	100.80(11)	98.84(13)	99.90 (8)	Cl1–Zn1–N1	92.69(7)	N1–Zn1–N4i	100.78(8)	99.18(13)
N2–Zn1–N4	75.45(14)	74.18(13)	74.70 (8)	Cl1–Zn1–N2	113.74(7)	N2–Zn1–N4	74.34(9)	74.28(14)
N2–Zn1–N5	93.52(12)	93.18(13)	93.01 (7)	Cl1–Zn1–N4	102.54 (6)	N2–Zn1–N1i	93.28(9)	93.06(15)
N2–Zn1–N6	160.95(13)	162.01(13)	161.45 (8)	Cl2–Zn1–N1	96.58(6)	N2–Zn1–N2i	161.53(10)	160.62(13)
N2–Zn1–N8	118.70(11)	119.42(13)	120.32 (8)	Cl2–Zn1–N2	126.11(7)	N2–Zn1–N4i	119.93(9)	120.55(14)
N4–Zn1–N5	98.27(12)	101.96(12)	97.52 (7)	Cl2–Zn1–N4	101.87(6)	N4–Zn1–N1i	100.78(8)	99.18(3)
N4–Zn1–N6	119.43(12)	119.63(13)	118.66 (8)	-	-	N4–Zn1–N2i	119.93(9)	120.55(14)
N4–Zn1–N8	88.86(11)	90.10(13)	91.23 (8)	-	-	N4–Zn1–N4i	88.96(9)	90.36(12)
N5–Zn1–N6	73.43(12)	73.36(13)	73.26 (7)	-	-	N1i–Zn1–N2i	73.29(9)	73.12(14)
N5–Zn1–N8	147.73(12)	147.32(13)	146.66 (8)	-	-	N1i–Zn1–N4i	146.79(9)	146.39(17)
N6–Zn1–N8	75.66(11)	74.27(13)	74.31 (8)	-	-	N2i–Zn1–N4i	74.34(9)	74.28(14)

\*symmetry operation i:  $1-x, y, 1/2-z$

## Description of crystal packings

In the crystal structure of **1-Cl**, the hydrogen-bonded centrosymmetric dimer is connected through the single H-interaction N3–H $\cdots$ Cl1<sup>a</sup> where azomethine nitrogen acts as a donor, and chloride from the neighboring molecule as an acceptor (Table S2, Figure S21A). Aromatic cycle stacking interaction (Cg1 $\cdots$ Cg1<sup>b</sup>) is formed between two phenyl rings from neighboring molecules (Table S2, Figure S21B), connecting centrosymmetric dimmers to form a chain parallel to the *c*-crystallographic axis.

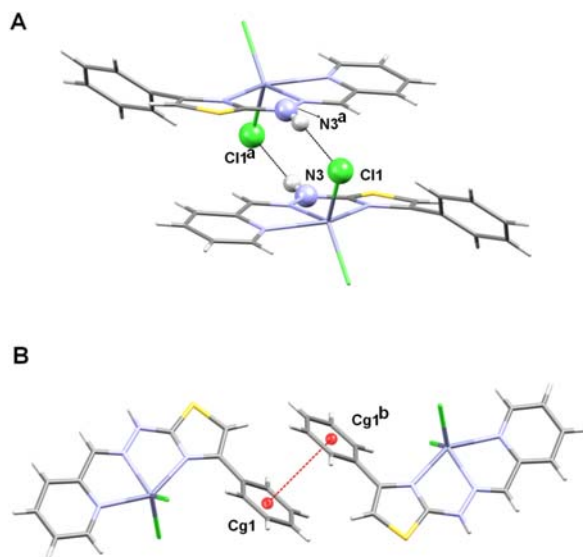


Figure S21. Hydrogen bond in the crystal structure (A) aromatic cycle stacking interactions (B) in the crystal structure of **1-Cl** showed as dashed lines (<sup>a</sup> = 1- $x$ , - $y$ , - $z$ ; <sup>b</sup> = 1- $x$ , - $y$ , 1- $z$ ).

Crystal packing of the isostructural complexes **2-Cl** and **3-Cl** is analogous, with the one difference: in **2-Cl** there is an additional non-classical C–H $\cdots$ Cg interaction (Figures S22–S24). Classical hydrogen interaction connects the azomethine nitrogen N3 as a donor to a Cl2<sup>c/i</sup> from the ZnCl4<sup>2-</sup> anion as an acceptor. In such a way an “endless” chain is formed stretching parallel to the *a*-crystallographic axis in the structure of **2-Cl** and **3-Cl** (Figure S22B and S23A, Table S2). The complexes share an identical crystal packing pattern of non-classical hydrogen and cycle aromatic interactions. Complex cations are double donors in non-classical hydrogen interactions through carbon atoms (C3 and C6), while chlorides (Cl2<sup>e/k</sup> and Cl1<sup>d/j</sup>) from two neighboring ZnCl4<sup>2-</sup> anions represent acceptors, which contribute to the formation of the 2-D network parallel to the *ac* crystallographic plane (Figure S22C and S23B, Table S2). Aromatic stacking interaction between pyridine and phenyl ring from neighboring molecules in **2-Cl** and **3-Cl** (Figure S22D and S24, Table S2), and C14–H $\cdots$ Cg interaction in **2-Cl** are responsible for the formation of “endless” chains parallel to *c*-crystallographic axis (Fig S22A, Table S2).

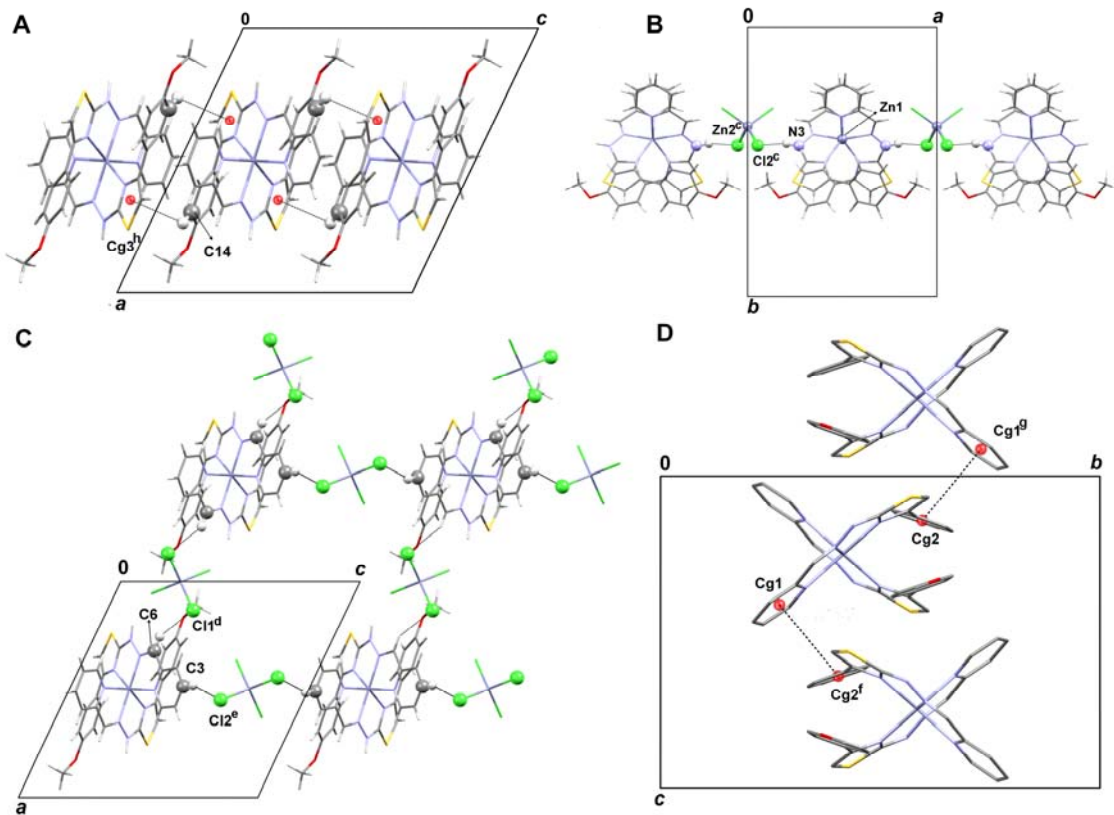


Figure S22. The crystal packing of **2-ClI**: C–H $\cdots$ Cg interactions (A); Classical hydrogen interactions (B); Non-classical interaction (C); Cg $\cdots$ Cg interactions (D). All interactions are shown as dashed lines (symmetry operations:  $c = -1/2+x, 1/2-y, 1/2+z$ ;  $d = 1-x, y, 1/2-z$ ;  $e = 3/2-x, 1/2-y, 1-z$ ;  $f = x, 1-y, 1/2+z$ ;  $g = x, 1-y, -1/2+z$ ;  $h = 1-x, 1-y, -z$ ).

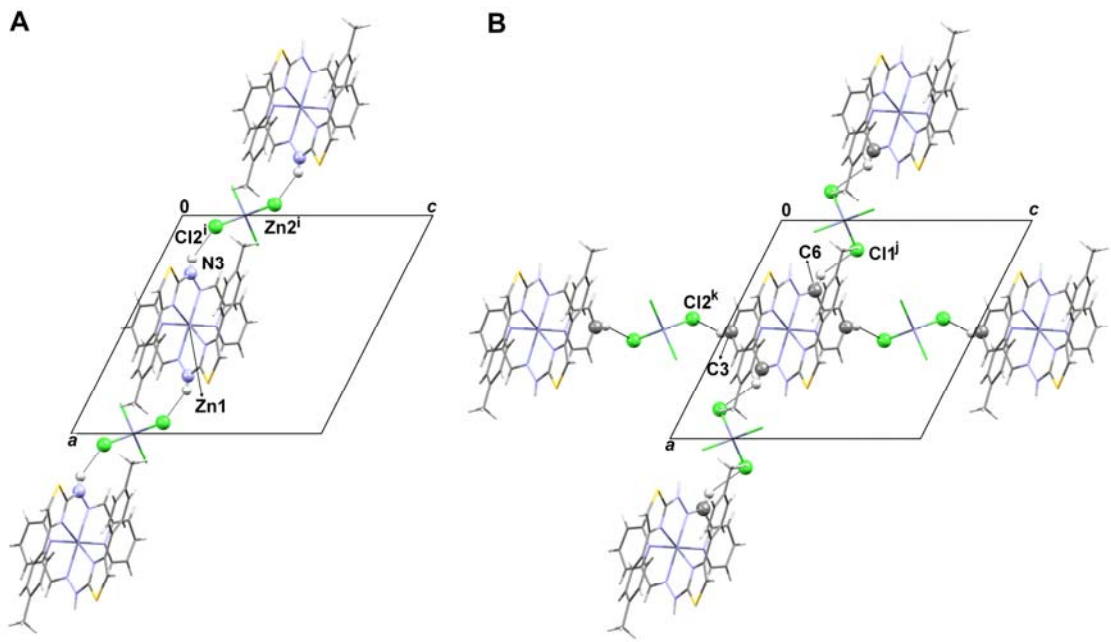


Figure S23. The crystal packing of **3-Cl**: Classical hydrogen interactions (A); Non-classical interactions (B). All interactions are shown as dashed lines (symmetry operations:  
 $i = 1-x, y, 1/2-z; j = -x, y, 1/2-z; k = 1/2+x, 1/2-y, -1/2+z$ ).

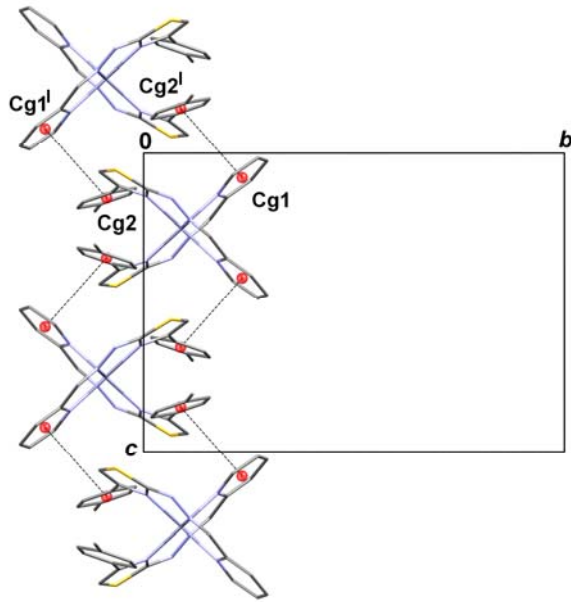


Figure S24.  $C_g \cdots C_g$  interactions in the crystal structure of **3-Cl** showed as dashed lines (symmetry operation  $l = 1-x, -y, -z$ ).

Table S2. Crystal packing parameters in the crystal structures of complexes 1–3-Cl.

Compound	Interactions parameters						
Hydrogen interactions parameters							
1-Cl	N-H···A		H···A (Å)	D···A (Å)	D-H···A (°)	sym. op. on A	
	N3-H···Cl1 <sup>a</sup>		2.37	3.1542(3)	167	1-x, -y, -z	
Aromatic cycle stacking parameters							
1-Cl	$\Omega(I), \Omega(J)^{A1}$	Cg···Cg <sup>B</sup> (Å)	$\alpha^C$ (°)	$\beta^D$ (°)	$\gamma^E$ (°)	slippage <sup>F</sup> (Å)	symmetry operation on J
	Cg1,Cg1 <sup>b</sup>	3.785(2)	0.00 (17)	15.1	15.1	0.989	1-x, -y, 1-z
Hydrogen interactions parameters							
2-Cl	N-H···A		H···A (Å)	D···A (Å)	D-H···A (°)	sym. op. on A	
	N3-H···Cl2 <sup>c</sup>		2.31	3.1124(1)	152	-1/2+x, 1/2-y, 1/2+z	
	C3-H···Cl2 <sup>c</sup>		2.80	3.694(3)	156	3/2-x, 1/2-y, 1-z	
	C6-H···Cl1 <sup>d</sup>		2.70	3.544(3)	148	1-x, y, 1/2-z	
Aromatic cycle stacking parameters							
2-Cl	$\Omega(I), \Omega(J)^{A2}$	Cg···Cg <sup>B</sup> (Å)	$\alpha^C$ (°)	$\beta^D$ (°)	$\gamma^E$ (°)	slippage <sup>F</sup> (Å)	symmetry operation on J
	Cg1,Cg2 <sup>f</sup>	3.947(2)	22.84 (13)	23.1	24.3	/	x, 1-y, 1/2 +z
	Cg2,Cg1 <sup>g</sup>	3.947(2)	22.84 (13)	24.3	23.1	/	x, 1-y, -1/2 +z
C–H...Cg interactions							
3-Cl	C–H... $\Omega(J)^G$	H...Cg	$\gamma^H$ (°)	C–H...Cg	C–H... $\pi$ angle	symmetry operation on J	
	C14-H...Cg3 <sup>h</sup>	2.99	10.99	116	3.508(3)	36	1-x, 1-y, -z
Hydrogen interactions parameters							
3-Cl	D-H···A		H···A (Å)	D···A (Å)	D-H···A (°)	sym. op. on A	
	N3-H···Cl2 <sup>i</sup>		2.37	3.1211(2)	144	1-x, y, 1/2-z	
	C3-H···Cl2 <sup>k</sup>		2.77	3.662(4)	158	1/2+x, 1/2-y, -1/2+z	
	C6-H···Cl1 <sup>j</sup>		2.69	3.516(5)	146	-x, y, 1/2-z	
Aromatic cycle stacking parameters							
3-Cl	$\Omega(I), \Omega(J)^{A3}$	Cg···Cg <sup>B</sup> (Å)	$\alpha^C$ (°)	$\beta^D$ (°)	$\gamma^E$ (°)	slippage <sup>F</sup> (Å)	symmetry operation on J
	Cg1,Cg2 <sup>l</sup>	4.075(2)	24.52(19)	22.5	28.6	/	1-x, -y, -z
	Cg2,Cg1 <sup>l</sup>	4.075(2)	24.52(19)	28.6	22.5	/	1-x, -y, -z

<sup>A1</sup>Planes of the rings I, J: ring  $\Omega(1) = C10-C11-C12-C13-C14-C15$ ; <sup>A2</sup> ring  $\Omega(1) = N1-C1-C2-C3-C4-C5$ ; ring  $\Omega(2) = C10-C11-C12-C13-C14-C15$ ; <sup>A3</sup> ring  $\Omega(1) = N1-C1-C2-C3-C4-C5$ ; ring  $\Omega(2) = C10-C11-C12-C13-C14-C15$ ;

<sup>B</sup> Cg···Cg = distance between ring centroids.

<sup>C</sup>  $\alpha$  = dihedral angle between planes I and J.

<sup>D</sup>  $\beta$  = angle between Cg(I)→Cg(J) vector and normal to plane I.

<sup>E</sup>  $\gamma$  = angle between Cg(I)→Cg(J) vector and normal to plane J.

<sup>F</sup> Slippage = distance between Cg(I) and perpendicular projection of Cg(J) on ring I.

<sup>G</sup> Center of gravity of ring J: ring  $\Omega(1) = S1-C7-N4-C8-C9$

<sup>H</sup>  $\gamma$  = angle between Cg-H vector and ring J normal

The complexes **1–3-NO<sub>3</sub>** have the same type of classical N–H···O interactions (Figures S25A, S26B and S27A, Table S3). In general, the complex cation is connected to both nitrate anions through two bifurcated H-interaction realized through the azomethine nitrogens as donors (N3 and N7) and nitrate oxygen atoms as acceptors. Also, the formation of non-classical H-interactions (C4–H···O3<sup>m</sup> and C17–H···O6<sup>o</sup> in **1-NO<sub>3</sub>**; C6–H···O6<sup>t</sup>, C21–H···O7<sup>t</sup> and C32–H···O5<sup>u</sup> in **3-NO<sub>3</sub>**) contribute to the formation of the 2-D supramolecular network parallel to (−5 5 3) crystallographic plane in **1-NO<sub>3</sub>** and *ab*-crystallographic plane in **3-NO<sub>3</sub>** (Figures S25A and S27A, respectively; Table S3). 2D supramolecular networks of **1-NO<sub>3</sub>** and **3-NO<sub>3</sub>** are connected *via* cycle aromatic stacking interactions (Cg3···Cg3<sup>o</sup> and Cg1···Cg1<sup>v</sup>, respectively) to form of 3D crystal packings. Additional C–H···Cg interactions (C18–H···Cg2<sup>o</sup>, C23–H···Cg2<sup>p</sup> and C26–H···Cg1<sup>p</sup>) in **1-NO<sub>3</sub>** and two non-classical H-interactions (realized through the C8 and C18 carbon atoms as donors and nitrate oxygens as acceptors) in **3-NO<sub>3</sub>**, contribute to the formation of 3D supramolecular structure of these complexes (Figures S25B and S27B, Table S3). In the case of **2-NO<sub>3</sub>**, described classical N–H···O and three non-classical H-interactions (through carbon atoms C16, C20, and C22) lead to the formation of 1-D-ladder like supramolecular structure, which lies in *bc*-crystallographic plane (Figure S26B, Table S3). The ladders are further connected *via* C8–H···Cg1<sup>s</sup> interactions to form a 2-D supramolecular network (Figure S26A, Table S3).

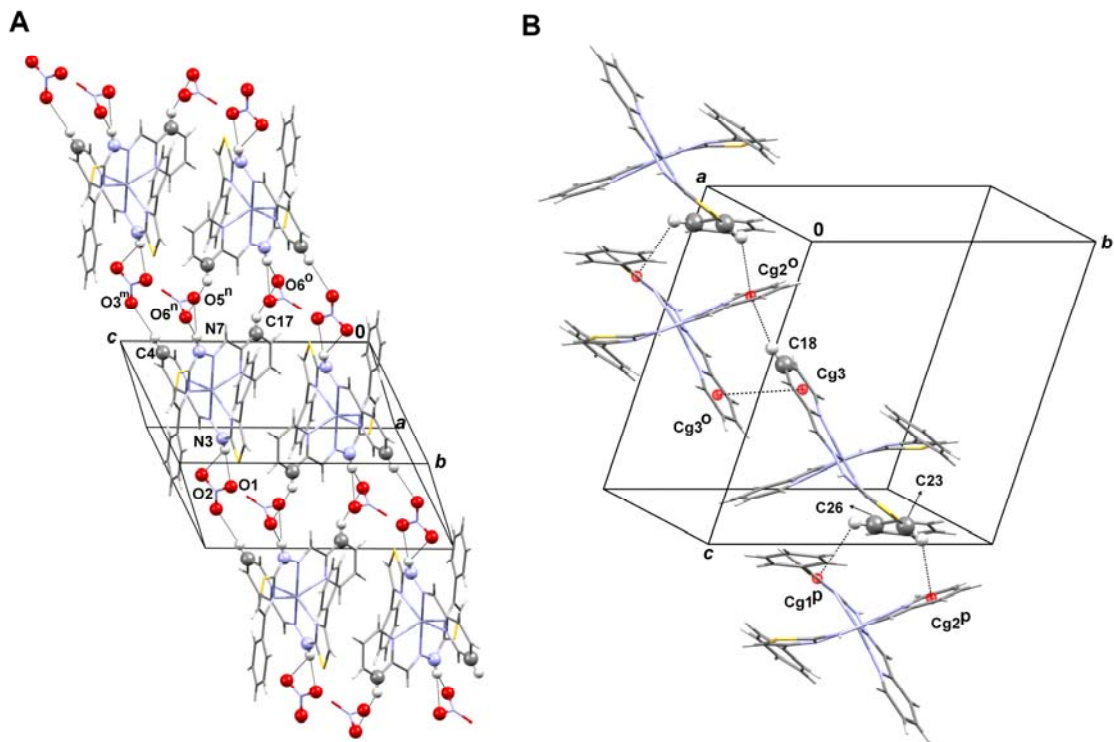


Figure S25. Crystal packing of **1-NO<sub>3</sub>**: Classical and non-classical hydrogen interactions (A); Cg···Cg and C-H···Cg interactions (B). All interactions are shown as dashed lines (symmetry operations: m = -1+x, -1+y, z; n = 1+x, y, z; o = -x, -y, 1-z; p = x, 1-y, 2-z).

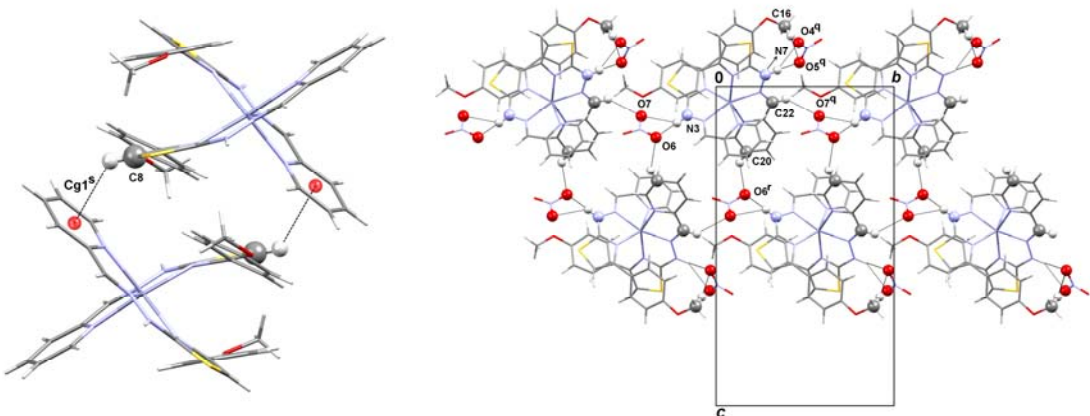


Figure S26. Crystal packing of **2-NO<sub>3</sub>**: C-H···Cg interactions (A); classical and non-classical hydrogen interaction (B). All interactions are shown as dashed lines (symmetry operations: q = x, 1+y, z; r = 2-x, 1/2+y, 1/2-z; s = 2-x, -y, -z).

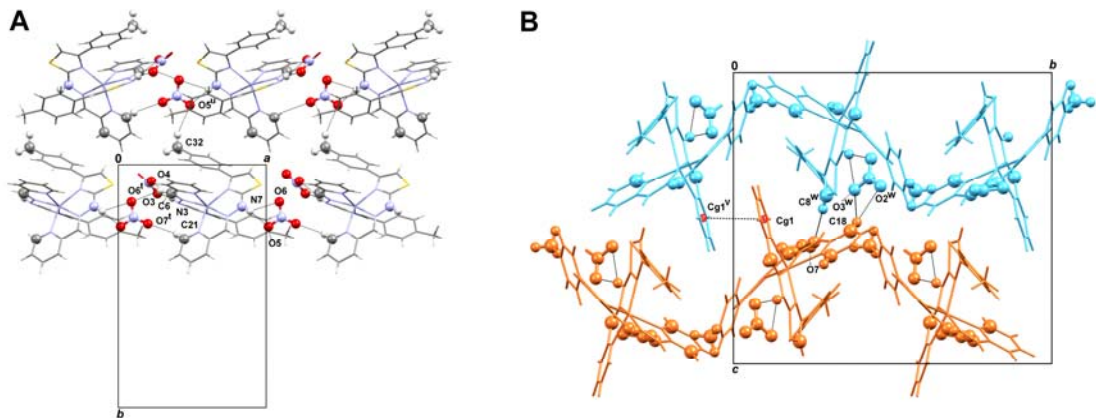


Figure S27. Crystal packing of **3-NO<sub>3</sub>**: Classical and non-classical hydrogen interactions (A); Cg···Cg and C–H···Cg interactions (B). All interactions are shown as dashed lines (symmetry operations: t = -1+x, y, z; u = 3/2-x, -1/2+y, 3/2-z; v = 1-x, -y, 1-z; w = 1/2+x, 1/2-y, -1/2+z).

Table S3. Crystal packing parameters in the crystal structures of complexes **1–3-NO<sub>3</sub>**.

Compound	Interactions parameters											
<b>1-NO<sub>3</sub></b>												
Hydrogen interactions parameters												
N-H···A	H···A (Å)	D···A (Å)	D-H···A (°)	sym. op. on A								
N3-H···O1	2.12	2.8491(1)	142	x,y,z								
N3-H···O2	2.31	2.9923(1)	136	x,y,z								
N7-H···O5 <sup>n</sup>	2.30	3.0849(1)	151	1+x,y,z								
N7-H···O6 <sup>n</sup>	1.90	2.7465(1)	148	1+x,y,z								
C4-H···O3 <sup>m</sup>	2.47	3.391(5)	169	-1+x,-1+y,z								
C17-H···O6 <sup>o</sup>	2.57	3.409(6)	150	-x,-y,1-z								
Aromatic cycle stacking parameters												
$\Omega(I)$ , $\Omega(J)^{A1}$	$Cg\cdots Cg^B$ (Å)	$\alpha^C$ (°)	$\beta^D$ (°)	$\gamma^E$ (°)	slippage <sup>F</sup> (Å)	symmetry operation on J						
Cg3,Cg3 <sup>o</sup>	3.787 (3)	0.0(2)	30.9	30.9	1.949	-x,-y,1-z						
C–H...Cg interactions												
C–H··· $\Omega(J)^{G1}$	H···Cg	$\gamma^E$ (°)	C–H...Cg	C...Cg	C–H...π angle	symmetry operation on J						
C18-H···Cg2 <sup>o</sup>	2.55	5.01	165	3.461 (5)	71	-x,-y,1-z						
C23-H···Cg2 <sup>p</sup>	2.70	8.66	138	3.453 (4)	57	x,1-y,2-z						
C26-H···Cg1 <sup>p</sup>	2.99	4.92	118	3.524 (4)	32	x,1-y,2-z						
<b>2-NO<sub>3</sub></b>												
Hydrogen interactions parameters												
N-H···A	H···A (Å)	D···A (Å)	D-H···A (°)	sym. op. on A								
N3-H···O6	2.09	2.8158(1)	142	x,y,z								
N3-H···O7	2.43	3.0890(1)	134	x,y,z								
N7-H···O4 <sup>q</sup>	2.35	3.1211(2)	149	x,1+y,z								
N7-H···O5 <sup>q</sup>	2.23	2.8990(1)	135	x,1+y,z								
C16-H···O5 <sup>q</sup>	2.59	3.532(7)	168	x,1+y,z								
C20-H···O6 <sup>r</sup>	2.53	3.327(6)	145	2-x,1/2+y,1/2-z								
C22-H···O7 <sup>q</sup>	2.58	3.316(5)	136	x,1+y,z								
C–H...Cg interactions												
C–H··· $\Omega(J)^{G2}$	H···Cg	$\gamma^H$ (°)	C–H...Cg	C...Cg	C–H...π angle	symmetry operation on J						
C8-H···Cg1 <sup>s</sup>	2.69	11.93	132	3.387(5)	54	2-x,-y,-z						
<b>3-NO<sub>3</sub></b>												
Hydrogen interactions parameters												
D-H···A	H···A (Å)	D···A (Å)	D-H···A (°)	sym. op. on A								
N3-H···O3	2.62	3.162 (1)	139	x,y,z								
N3-H···O4	2.16	2.829 (4)	169 (4)	x,y,z								
N7-H···O5	2.04	2.797(3)	169 (4)	x,y,z								
N7-H···O6	2.47	3.054(3)	134(3)	x,y,z								
C6-H···O6 <sup>t</sup>	2.49	3.232(3)	137	-1+x,y,z								
C8 <sup>w</sup> -H···O7	2.38	3.209(4)	148	1/2+x,1/2-y,-1/2+z								
C18-H···O2 <sup>w</sup>	2.57	3.319(4)	138	1/2+x,1/2-y,-1/2+z								
C18-H···O3 <sup>w</sup>	2.54	3.380(4)	151	1/2+x,1/2-y,-1/2+z								
C21-H···O7 <sup>t</sup>	2.51	3.112(3)	122	-1+x,y,z								
C32-H···O5 <sup>u</sup>	2.58	3.474(5)	156	3/2-x,-1/2+y,3/2-z								
Aromatic cycle stacking parameters												
$\Omega(I)$ , $\Omega(J)^{A2}$	$Cg\cdots Cg^B$ (Å)	$\alpha^C$ (°)	$\beta^D$ (°)	$\gamma^E$ (°)	Slippage <sup>F</sup> (Å)	symmetry operation on J						
Cg1,Cg1 <sup>v</sup>	3.8735 (18)	0.00	18.9	18.9	1.256	1-x,-y,1-z						

<sup>A1</sup>Planes of the rings I, J: ring  $\Omega(1) = N5-C16-C17-C18-C19-C20$ ; <sup>A2</sup> ring  $\Omega(1) = N1-C1-C2-C3-C4-C5$ ;

<sup>B</sup>  $Cg\cdots Cg$  = distance between ring centroids.

<sup>C</sup>  $\alpha$  = dihedral angle between planes I and J.

<sup>D</sup>  $\beta$  = angle between  $Cg(I)\rightarrow Cg(J)$  vector and normal to plane I.

<sup>E</sup>  $\gamma$  = angle between  $Cg(I)\rightarrow Cg(J)$  vector and normal to plane J.

<sup>F</sup> Slippage = distance between  $Cg(I)$  and perpendicular projection of  $Cg(J)$  on ring I.

<sup>G1</sup> Center of gravity of ring J: ring  $\Omega(1) = N8-C22-S2-C23-C24$ ; ring  $\Omega(2) = N1-C1-C2-C3-C4-C5$ ; <sup>G2</sup> ring  $\Omega(1) = N5-C17-C18-C19-C20-C21$ ;

<sup>H</sup>  $\gamma$  = angle between  $Cg-H$  vector and ring J normal

## Phase purity

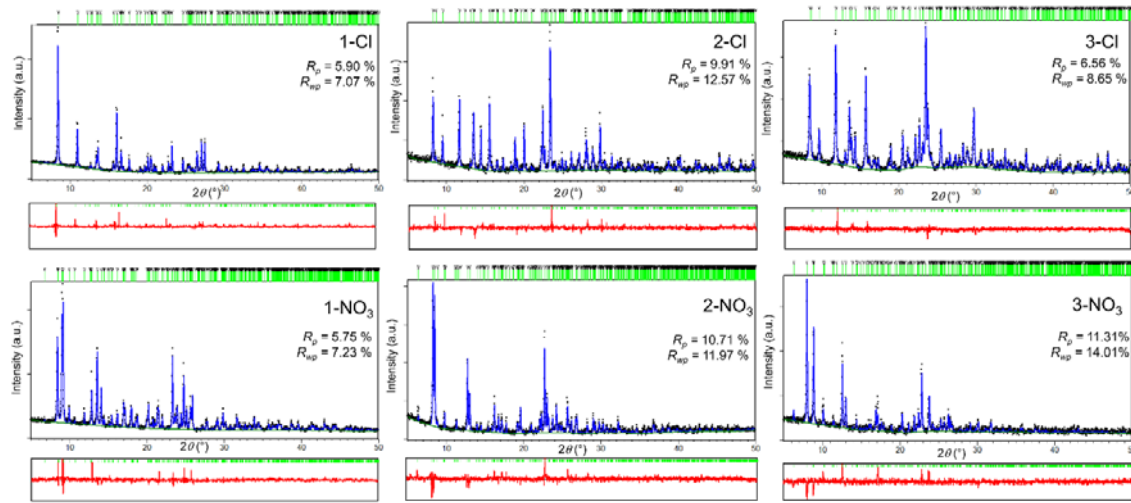


Figure S28. Rietveld refinements on samples **1–3-Cl** and **1–3-NO<sub>3</sub>**. Experimental data are given by black dots, the calculated pattern is shown in blue while the red line represents the difference curve. Green vertical marks show the positions of diffraction reflections.

### 3. Hirshfeld analysis

In all complexes, the interactions can be observed as the Hirshfeld three-dimensional shape-index plot (as red and blue relief regions) and in the curvature plot as a flat zone, in the same position of the surface as in the shape-index plot mapped on the complex cations.

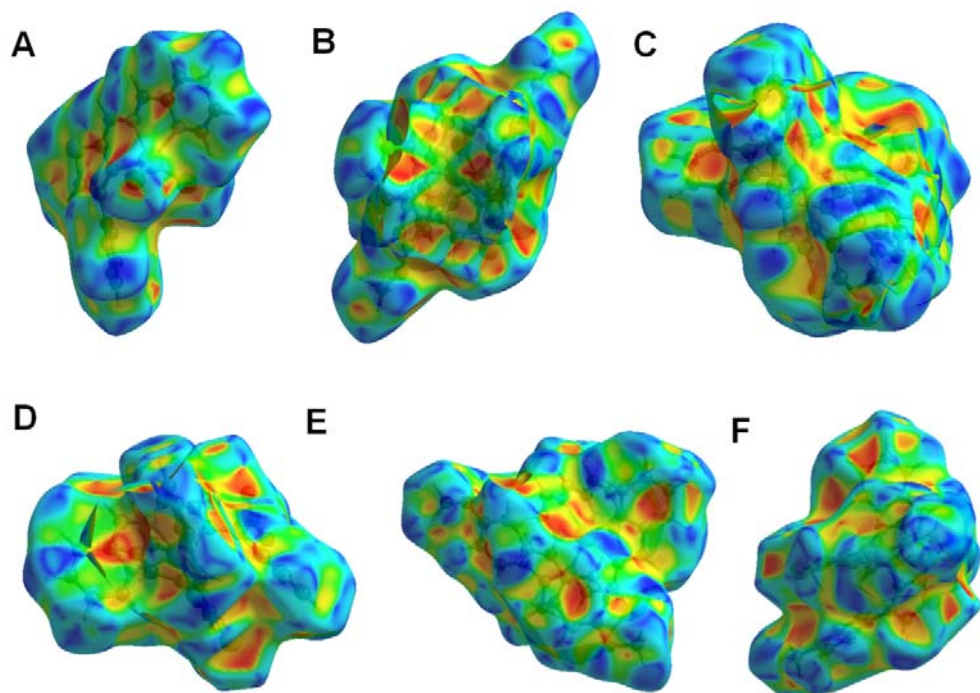


Figure S29. Shape index plots of **1–3-Cl** (A–C) and **1–3-NO<sub>3</sub>** (D–F).

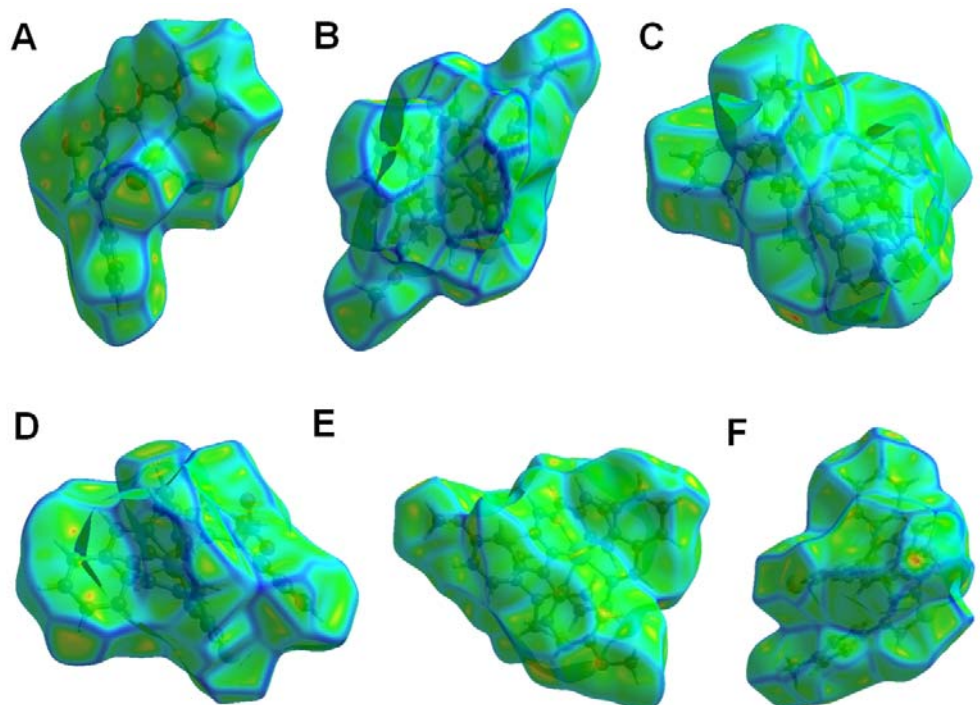


Figure S30. Curvedness plots of **1–3-Cl** (A–C) and **1–3-NO<sub>3</sub>** (D–F).

Values of  $di$  and  $de$  for selected interactions with significant contributions are given in Table S4. The nearest nucleus external to the surface is denoted by  $de$ , and the distance from the surface to the nearest nucleus internal to the surface is denoted by  $di$ .

Table S4. Values of  $di/de$  for selected interactions in the crystal structures of **1-3-Cl** and **1-3-NO<sub>3</sub>**.

Interaction number	Interaction type	<b>1-Cl</b>	<b>2-Cl</b>	<b>3-Cl</b>
1	H···Cl	1.4 / 0.8	0.8 / 1.4	0.8 / 1.4
2	H···C	1.7 / 1.35	1.6 / 1.1	1.7 / 1.1
3	H···S	1.7 / 1.1	1.8 / 1.1	1.8 / 1.1
4	H···O	-	1.2 / 1.7	-
5	C···C	1.6 / 1.7	1.6 / 1.7	1.6 / 1.7
6	H···N	1.7 / 1.3	1.7 / 1.2	1.8 / 1.5
Interaction number	Interaction type	<b>1-NO<sub>3</sub></b>	<b>2-NO<sub>3</sub></b>	<b>3-NO<sub>3</sub></b>
1	H···Cl	-	-	-
2	C···H	1.6 / 1.0	1.6 / 1.0	1.6 / 1.0
3	S···H	1.8 / 1.1	1.7 / 1.1	1.9 / 1.1
4	H···O	0.7 / 1.1	0.8 / 1.2	0.8 / 1.1
5	C···C	1.6 / 1.7	1.6 / 1.7	1.6 / 1.7
6	H···N	0.8 / 1.4	1.1 / 1.5	/ 1.6

## 4. Intermolecular interaction energies and energy frameworks

Table S5. – Illustrations of orientations, corresponding interactions and interaction energies (in kcal/mol), used to describe the packing in the crystal structure of **1-Cl**

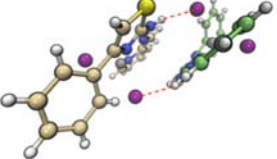
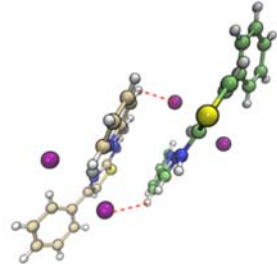
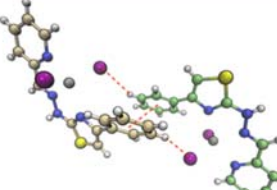
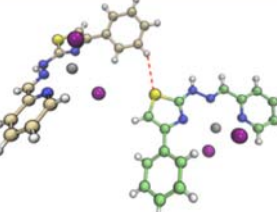
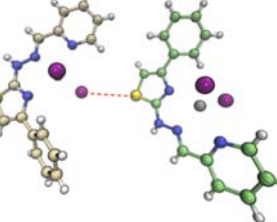
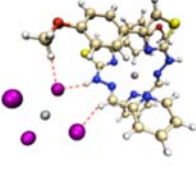
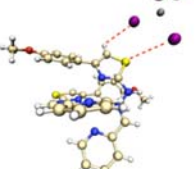
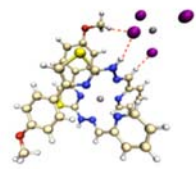
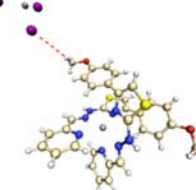
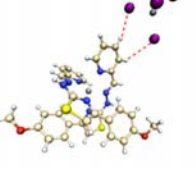
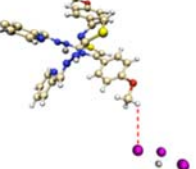
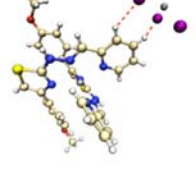
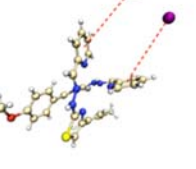
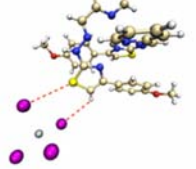
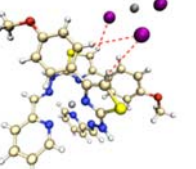
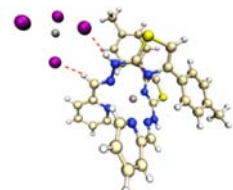
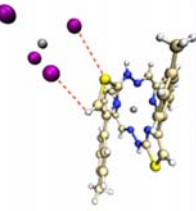
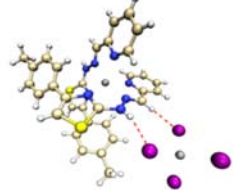
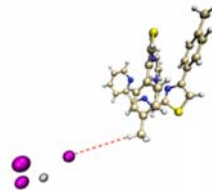
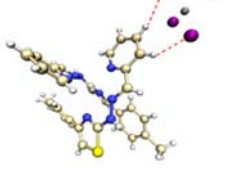
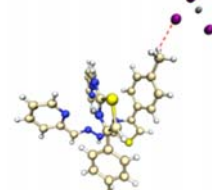
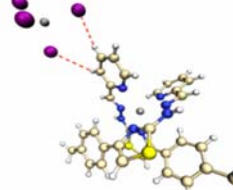
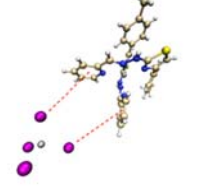
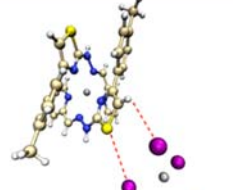
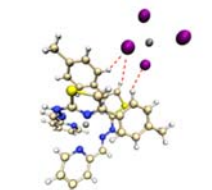
	Orientation	Interactions	Interaction Energy (kcal/mol)
1		N–H···Cl Cl···H–N	-25.1
2		C–H···Cl Cl···H–C	-13.8
3		$\pi\cdots\pi$ Cl···H–C C–H···Cl	-4.1
4		S···H–C	-3.2
5		Cl···S	-1.3

Table S6. – Illustrations of orientations, corresponding interactions and interaction energies (in kcal/mol), used to describe the packing in the crystal structure of 2-Cl

	Orientation	Interactions	Interaction Energy (kcal/mol)		Orientation	Interactions	Interaction Energy (kcal/mol)
1		Cl···H-C Cl···H-N Cl···H-C	-222.6	3A		C-H···Cl S···Cl	-177.1
1A*		C-H···Cl N-H···Cl C-H···Cl	-222.6	4		Cl···H-C	-149.9
2		C-H···Cl C-H···Cl	-180.7	4A		C-H···Cl	-149.9
2A		C-H···Cl C-H···Cl	-180.7	5		$\pi\cdots\text{Cl}$ $\pi\cdots\text{Cl}$ 6.2 Å	-163.5
3		Cl···S Cl···H-C	-177.1	6		C-H···Cl C-H···Cl C-H···Cl	-186.2

\*Interactions denoted with the letter A are duplicated due to symmetry.

Table S7. Illustrations of orientations, corresponding interactions and interaction energies (in kcal/mol), used to describe the packing in the crystal structure of **3-Cl**

	Orientation	Interactions	Interaction Energy (kcal/mol)		Orientation	Interactions	Interaction Energy (kcal/mol)
1		Cl···H-N Cl···H-C	-218.2	3A		Cl···S Cl···H-C	-181.6
1A *		N-H···Cl C-H···Cl	-218.2	4		Cl···H-C	-147.5
2		C-H···Cl C-H···Cl	-180.6	4A		C-H···Cl	-147.5
2A		Cl···H-C Cl···H-C	-180.6	5		Cl···π Cl···π	-164.6
3		C-H···Cl S···Cl	-181.6	6		C-H···Cl C-H···Cl C-H···Cl	-188.8

\*Interactions denoted with the letter A are duplicated due to symmetry.

Table S8 – Illustrations of orientations, corresponding interactions and interaction energies (in kcal/mol), used to describe the packing in the crystal structure of **1**– $\text{NO}_3$

	Orientation	Interactions	Interaction Energy (kcal/mol)		Orientation	Interactions	Interaction Energy (kcal/mol)
1		N–H…O	–135.8	8		O…H–C O…H–C	–7.3
2		N–H…O	–137.6	9		O…H–C	–1.7
3		C–H…O	–103.2	10		C–H…O C–H…O	–115.4
4		C–H…O	–108.6	11		C–H…O C–H…O	–115.2
5		O…H–C O…H–C	–6.1	12		C–H…O C–H…O	–104.8
6		C–H…O C–H…O	–116.2	13		C–H…O	–94.5
7		C–H…O	–97.9				

Table S9 – Illustrations of orientations, corresponding interactions and interaction energies (in kcal/mol), used to describe the packing in the crystal structure **2-NO<sub>3</sub>**

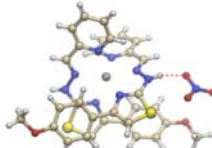
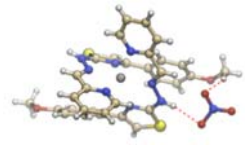
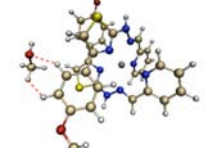
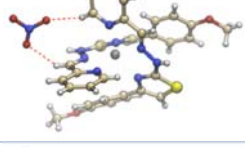
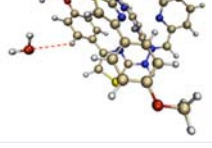
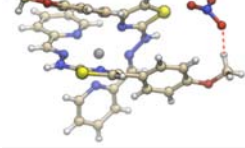
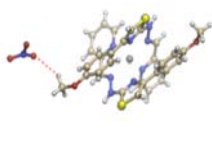
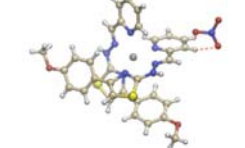
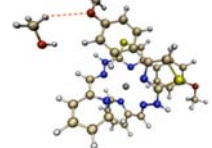
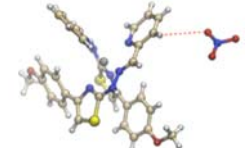
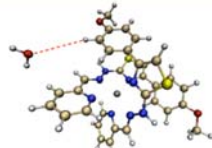
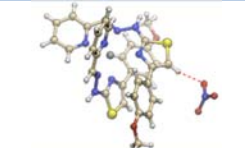
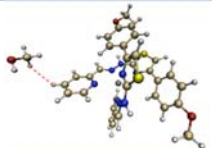
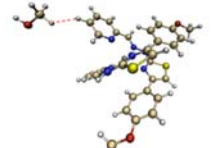
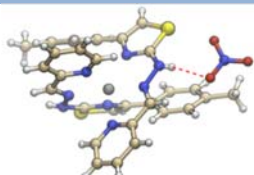
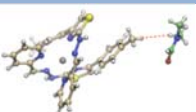
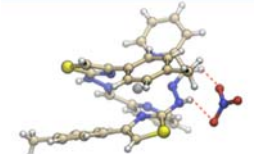
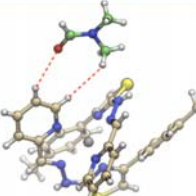
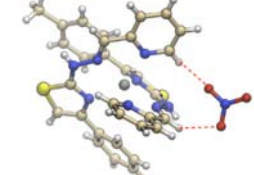
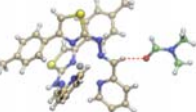
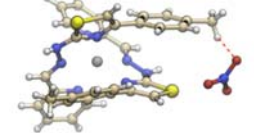
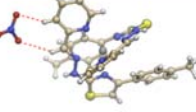
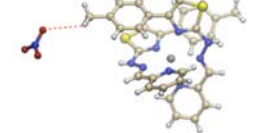
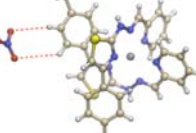
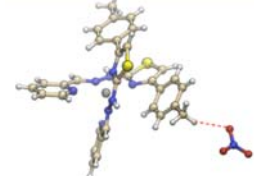
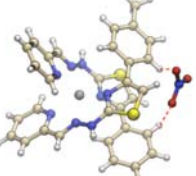
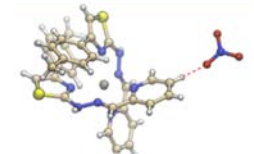
	<b>Orientation</b>	<b>Interactio ns</b>	<b>Interactio n Energy (kcal/mol)</b>		<b>Orientation</b>	<b>Interactio ns</b>	<b>Interactio n Energy (kcal/mol)</b>
1		N–H···O	-132.7	9		O···H–C	-26.3
2		N–H···O C–H···O	-138.9	10		$\sigma\cdots\sigma$ O···H–C	-19.8
3		O···H–C O···H–C	-122.8	11		O···H–C	-20.3
4		C–H···O	-112.5	12		O···H–C	-91.5
5		C–H···O C–H···O	-117.2	13		C–H···O	-17.6
6		C–H···O	-99.3	14		O···H–C	-20.0
7		C–H···O	-102.8	15		H···H	-14.7
8		C–H···S	-18.1	16		H···H	-17.0

Table S10 – Illustrations of orientations, corresponding interactions and interaction energies (in kcal/mol), used to describe the packing in the crystal structure **3-NO<sub>2</sub>**

	Orientation	Interactions	Interaction Energy (kcal/mol)		Orientation	Interactions	Interaction Energy (kcal/mol)
1		N–H···O	-133.7	8		H···H	-2.2
2		N–H···O C–H···O	-135.5	9		H···H C–H···O	-8.4
3		C–H···O C–H···O	-127.5	10		C–H···O	-14.9
4		C–H···O	-110.4	11		O···H–C O···H–C	-112.6
5		O···H–C	-86.6	12		O···H–C O···H–C	-95.2
6		C–H···O	-93.9	13		C–H···O	-105.8
7		C–H···O	-99.8				

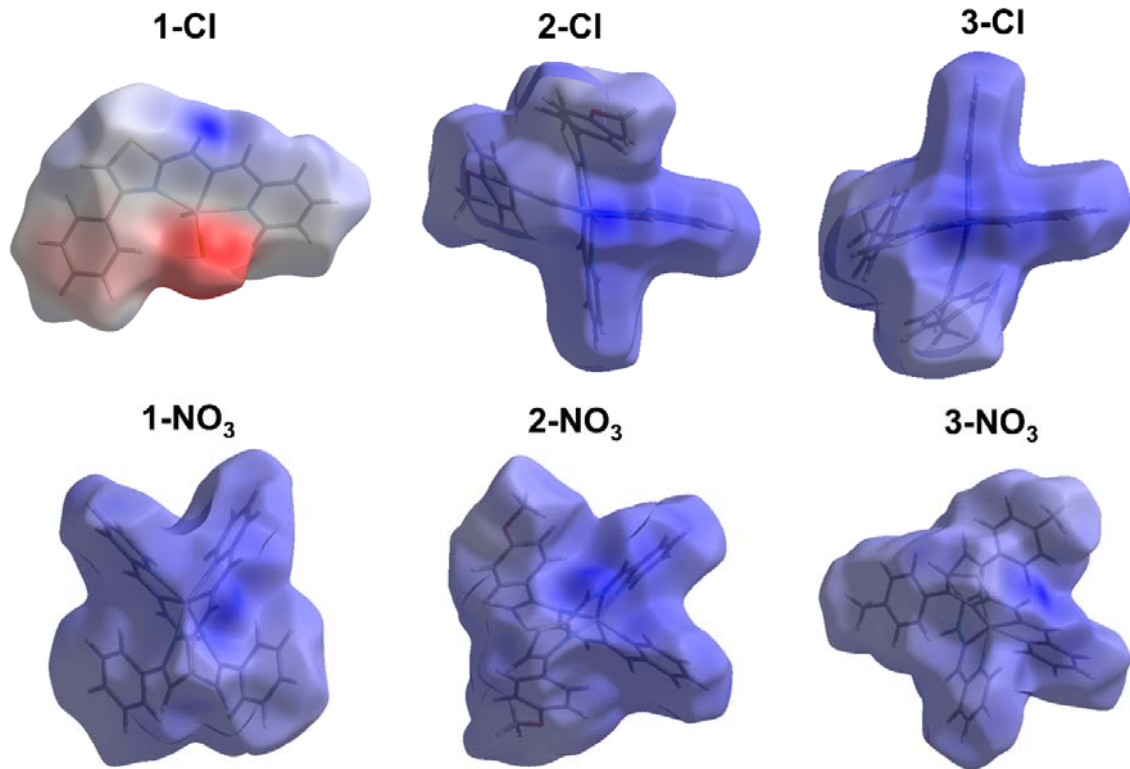


Figure S31. Electrostatic potential maps mapped on the Hirshfeld surface for all complexes.

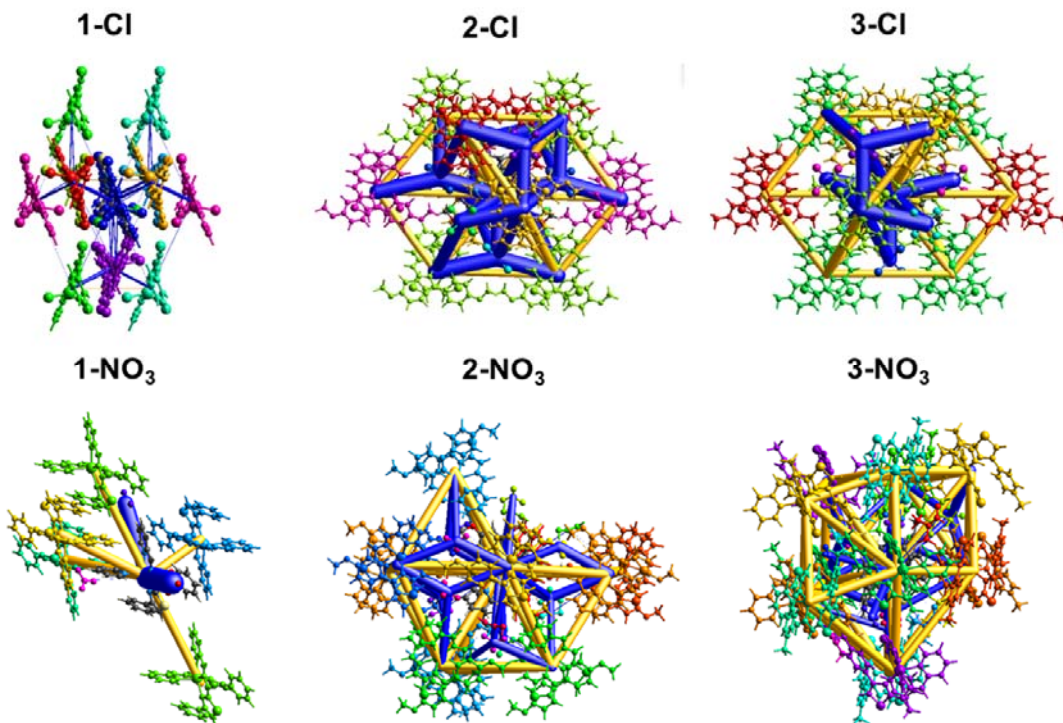


Figure S32. Total energy-framework diagrams for a cluster of nearest-neighbour molecules of investigated complexes **1–3-Cl** and **1–3-NO<sub>3</sub>**. All diagrams use the same cylinder scale of 10 for energies (blue cylinders for total and yellow cylinders for positive destabilizing energies).

Table S11. Energy of interactions of pairs of molecules in the crystal structure of **1-Cl** based on B3LYP/DGDZVP energy model

	N	Symop	R	Electron Density	E_ele	E_pol	E_dis	E_rep	E_tot
Red	1	-x, -y, -z	5.64	B3LYP/DGDZVP	-171.2	-49.3	-80.5	174.2	-180.0
Orange	1	-x, -y, -z	6.69	B3LYP/DGDZVP	-92.5	-24.5	-82.6	98.4	-127.1
Yellow	1	-x, -y, -z	11.14	B3LYP/DGDZVP	-7.3	-3.4	-31.4	28.2	-20.2
Green	2	-x, y+1/2, -z+1/2	9.50	B3LYP/DGDZVP	-15.9	-5.0	-13.0	17.9	-20.8
Cyan	2	-x, y+1/2, -z+1/2	8.91	B3LYP/DGDZVP	-3.7	-3.5	-9.7	4.0	-12.5
Blue	1	-x, -y, -z	9.46	B3LYP/DGDZVP	-28.5	-11.2	-29.9	38.3	-40.8
Dark Blue	2	x, y, z	14.15	B3LYP/DGDZVP	-0.2	-1.5	-8.6	5.3	-5.5
Purple	2	x, -y+1/2, z+1/2	9.54	B3LYP/DGDZVP	-39.7	-12.5	-30.8	37.3	-55.0
Magenta	2	x, y, z	7.41	B3LYP/DGDZVP	20.6	-6.0	-9.5	1.9	10.3

\*Total energy (E\_tot) represent the sum of individual components with scaling factors ( $k_{ele} = 1.057$ ;  $k_{pol} = 0.740$ ;  $k_{dis} = 0.871$ ;  $k_{rep} = 0.618$ ), while individual components are not scaled. For color code see Figure S31.

Table S12. Energy of interactions of pairs of molecules in the crystal structure of **2-Cl** based on B3LYP/DGDZVP energy model

	N	Symop	R	Electron Density	E_ele	E_pol	E_dis	E_rep	E_tot
Red	2	-x+1/2, -y+1/2, -z	11.25	B3LYP/DGDZVP	574.4	-58.5	-18.0	4.0	550.9
Orange	2	-x, -y, -z	7.34	B3LYP/DGDZVP	548.4	-76.5	-123.8	127.8	494.3
Yellow	4	x+1/2, y+1/2, z	11.73	B3LYP/DGDZVP	481.2	-43.1	-32.5	24.5	463.7
Green	2	-	8.27	B3LYP/DGDZVP	-618.0	-72.6	-10.0	13.1	-707.7
Cyan	1	-	7.36	B3LYP/DGDZVP	-667.3	-132.3	-27.1	35.4	-805.2
Blue	2	-	7.45	B3LYP/DGDZVP	-862.4	-163.1	-30.7	103.5	-995.2
Purple	2	-	9.60	B3LYP/DGDZVP	-648.4	-70.3	-12.6	22.0	-734.8
Magenta	2	x, y, z	14.41	B3LYP/DGDZVP	408.1	-21.4	-12.5	11.9	412.0

\*Total energy (E\_tot) represent the sum of individual components with scaling factors ( $k_{ele} = 1.057$ ;  $k_{pol} = 0.740$ ;  $k_{dis} = 0.871$ ;  $k_{rep} = 0.618$ ), while individual components are not scaled. For color code see Figure S31.

Table S13. Energy of interactions of pairs of molecules in the crystal structure of **3-Cl** based on B3LYP/DGDZVP energy model

	N	Symop	R	Electron Density	E_ele	E_pol	E_dis	E_rep	E_tot
	2	x, y, z	14.33	B3LYP/DGDZVP	399.8	-18.0	-7.4	4.9	406.1
	2	-x+1/2, -y+1/2, -z	10.74	B3LYP/DGDZVP	587.7	-66.3	-24.4	8.6	556.3
	2	-x, -y, -z	7.46	B3LYP/DGDZVP	549.2	-69.5	-109.0	106.7	500.1
	4	x+1/2, y+1/2, z	11.60	B3LYP/DGDZVP	492.2	-46.8	-34.2	26.9	472.7
	2	-	8.16	B3LYP/DGDZVP	-641.7	-79.6	-11.8	19.6	-735.6
	1	-	7.56	B3LYP/DGDZVP	-679.4	-129.0	-24.4	28.1	-817.7
	2	-	9.49	B3LYP/DGDZVP	-648.4	-71.6	-13.1	24.9	-734.6
	2	-	7.33	B3LYP/DGDZVP	-839.8	-161.5	-28.9	92.6	-975.4

\*Total energy (E\_tot) represent the sum of individual components with scaling factors ( $k_{ele} = 1.057$ ;  $k_{pol} = 0.740$ ;  $k_{dis} = 0.871$ ;  $k_{rep} = 0.618$ ), while individual components are not scaled. For color code see Figure S31.

Table S14. Energy of interactions of pairs of molecules in the crystal structure of **1-NO<sub>3</sub>** based on B3LYP/DGDZVP energy model

	N	Symop	R	Electron Density	E_ele	E_pol	E_dis	E_rep	E_tot
	1	-	6.21	B3LYP/DGDZVP	-989.8	-284.1	-16.7	68.2	-1229.1
	1	-x, -y, -z	10.89	B3LYP/DGDZVP	572.5	-69.0	-67.0	84.7	548.2
	2	x, y, z	12.58	B3LYP/DGDZVP	459.9	-33.1	-10.2	1.6	453.8
	1	-x, -y, -z	11.52	B3LYP/DGDZVP	526.8	-42.9	-6.5	0.1	519.6
	1	-x, -y, -z	7.11	B3LYP/DGDZVP	560.4	-81.1	-105.7	103.1	504.1
	1	-	8.63	B3LYP/DGDZVP	-721.1	-100.7	-4.3	11.3	-833.8
	1	-	7.03	B3LYP/DGDZVP	-2.6	-6.4	-14.4	19.8	-7.8

\*Total energy (E\_tot) represent the sum of individual components with scaling factors ( $k_{ele} = 1.057$ ;  $k_{pol} = 0.740$ ;  $k_{dis} = 0.871$ ;  $k_{rep} = 0.618$ ), while individual components are not scaled. For color code see Figure S31.

Table S15. Energy of interactions of pairs of molecules in the crystal structure of **2-NO<sub>3</sub>** based on B3LYP/DGDZVP energy model

	N	Symop	R	Electron Density	E_ele	E_pol	E_dis	E_rep	E_tot
1	1	-x, -y, -z	7.67	B3LYP/DGDZVP	534.8	-68.2	-93.7	82.8	484.5
1	1	-x, -y, -z	14.93	B3LYP/DGDZVP	342.3	-14.4	-17.6	17.5	346.7
2	1	x, y, z	11.92	B3LYP/DGDZVP	500.1	-50.7	-23.9	20.0	482.8
1	1	-x, -y, -z	6.96	B3LYP/DGDZVP	562.9	-87.2	-116.9	114.6	499.6
1	1	-	6.94	B3LYP/DGDZVP	-394.3	-58.6	-17.9	22.2	-462.2
1	1	-	8.60	B3LYP/DGDZVP	-298.2	-27.7	-4.7	6.3	-336.0
1	1	-	6.46	B3LYP/DGDZVP	-10.9	-6.4	-12.8	12.1	-19.9
1	1	-	9.35	B3LYP/DGDZVP	5.7	-4.3	-5.6	3.1	-0.1
2	2	-x, y+1/2, -z+1/2	12.46	B3LYP/DGDZVP	516.4	-42.0	-10.4	3.4	508.0
1	1	-	8.34	B3LYP/DGDZVP	-387.3	-36.6	-9.0	11.5	-437.3
1	1	-	6.17	B3LYP/DGDZVP	-511.1	-98.6	-25.6	79.2	-586.7
1	1	-	8.24	B3LYP/DGDZVP	1.2	-4.1	-4.3	1.1	-4.8
1	1	-	8.95	B3LYP/DGDZVP	14.4	-4.6	-4.9	2.8	9.3
2	2	x, -y+1/2, z+1/2	12.24	B3LYP/DGDZVP	471.9	-36.6	-37.8	35.8	461.0
1	1	-x, -y, -z	12.97	B3LYP/DGDZVP	485.4	-42.9	-19.2	11.7	472.0
1	1	-	6.27	B3LYP/DGDZVP	-508.4	-88.5	-22.6	58.4	-586.6
1	1	-	7.54	B3LYP/DGDZVP	25.5	-4.7	-5.0	3.3	21.2
1	1	-	6.93	B3LYP/DGDZVP	-449.0	-60.7	-13.6	18.1	-520.3
1	1	-	8.73	B3LYP/DGDZVP	-37.2	-6.5	-5.1	7.6	-43.8
1	1	-	8.65	B3LYP/DGDZVP	-360.8	-28.8	-6.2	9.7	-402.2
1	1	-	9.14	B3LYP/DGDZVP	-309.2	-25.6	-5.4	6.6	-346.5
1	1	-	8.62	B3LYP/DGDZVP	-346.7	-28.0	-4.2	2.7	-389.3
1	1	-	9.77	B3LYP/DGDZVP	-10.9	-2.0	-1.4	0.2	-14.2

\*Total energy (E\_tot) represent the sum of individual components with scaling factors ( $k_{ele} = 1.057$ ;  $k_{pol} = 0.740$ ;  $k_{dis} = 0.871$ ;  $k_{rep} = 0.618$ ), while individual components are not scaled. For color code see Figure S31.

Table S16. Energy of interactions of pairs of molecules in the crystal structure of **3-NO<sub>3</sub>** based on B3LYP/DGDZVP energy model

	N	Symop	R	Electron Density	E_ele	E_pol	E_dis	E_rep	E_tot
	1	-	10.13	B3LYP/DGDZVP	20.6	-7.1	-4.4	0.6	13.1
	1	-x, -y, -z	9.92	B3LYP/DGDZVP	542.9	-66.9	-48.6	27.3	499.0
	2	-x+1/2, y+1/2, -z+1/2	9.91	B3LYP/DGDZVP	493.5	-46.5	-36.5	20.8	468.4
	2	-x+1/2, y+1/2, -z+1/2	13.42	B3LYP/DGDZVP	418.7	-23.5	-7.6	6.3	422.6
	1	-	7.61	B3LYP/DGDZVP	5.5	-6.0	-11.8	12.6	-1.2
	1	-	7.71	B3LYP/DGDZVP	-45.2	-15.7	-15.2	15.3	-63.2
	1	-	9.66	B3LYP/DGDZVP	-289.5	-28.5	-5.8	9.9	-326.0
	1	-x, -y, -z	12.51	B3LYP/DGDZVP	419.9	-30.8	-26.9	20.8	410.6
	1	-	8.64	B3LYP/DGDZVP	-307.7	-25.4	-3.8	1.9	-346.3
	2	x+1/2, -y+1/2, z+1/2	10.49	B3LYP/DGDZVP	521.1	-49.9	-42.1	26.2	493.6
	1	-x, -y, -z	15.20	B3LYP/DGDZVP	417.6	-22.5	-5.6	3.1	421.9
	2	x, y, z	11.75	B3LYP/DGDZVP	486.9	-38.3	-10.1	1.1	478.4
	1	-	6.61	B3LYP/DGDZVP	19.4	-7.8	-22.5	13.8	3.6
	1	-	7.04	B3LYP/DGDZVP	-24.1	-13.9	-15.4	9.7	-43.2
	1	-	6.21	B3LYP/DGDZVP	-519.7	-95.2	-22.0	83.1	-587.7
	1	-	8.96	B3LYP/DGDZVP	-337.3	-28.1	-5.5	7.2	-377.8
	1	-	8.13	B3LYP/DGDZVP	-404.1	-43.7	-9.0	17.7	-456.5
	1	-	6.51	B3LYP/DGDZVP	-467.0	-70.5	-16.3	31.8	-540.5
	2	x+1/2, -y+1/2, z+1/2	11.72	B3LYP/DGDZVP	477.6	-32.8	-5.7	0.4	476.0
	1	-	7.14	B3LYP/DGDZVP	-367.3	-41.8	-9.9	24.1	-413.0
	1	-	10.08	B3LYP/DGDZVP	-6.7	-4.4	-7.3	2.9	-14.9
	1	-	7.01	B3LYP/DGDZVP	-382.9	-51.9	-13.7	17.3	-444.6
	1	-	6.16	B3LYP/DGDZVP	-525.2	-96.7	-21.2	92.5	-588.2

\*Total energy (E\_tot) represent the sum of individual components with scaling factors ( $k_{\text{ele}} = 1.057$ ;  $k_{\text{pol}} = 0.740$ ;  $k_{\text{dis}} = 0.871$ ;  $k_{\text{rep}} = 0.618$ ), while individual components are not scaled. For color code see Figure S31.

## 5. Thermal stability

After oxidative degradation of all complexes, the final residue was analyzed by FTIR spectroscopy. The FTIR spectra of the crude residues are given in Figure S31.

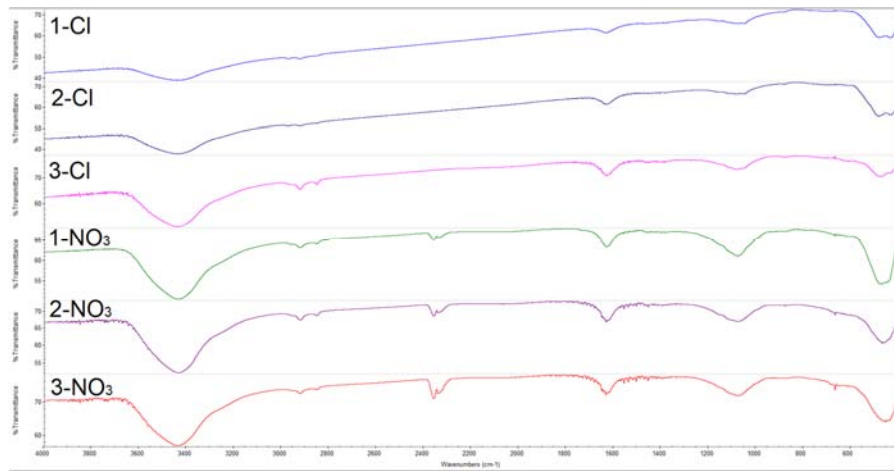


Figure S33. IR spectra of final residues of oxidative decomposition of all complexes.

## 6. Photoluminescence and DFT and TD-DFT computational study

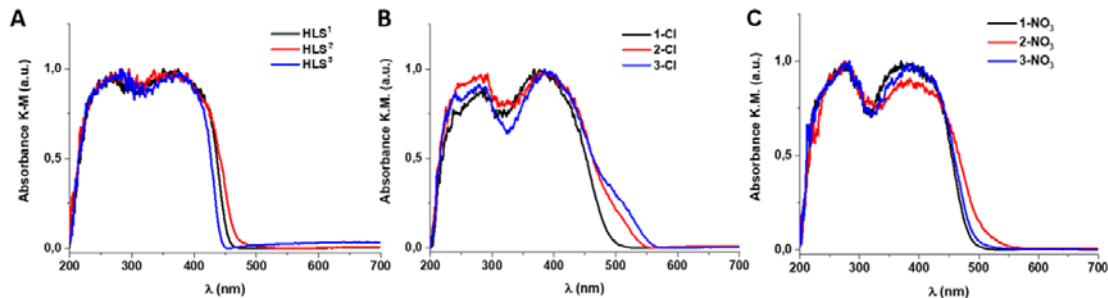


Figure S34. Solid state absorption spectra for the free ligands **HLS**<sup>1–3</sup> (A), chloride-based complexes **1–3-Cl** (B) and nitrate-based complexes **1–3-NO<sub>3</sub>** (C). Black line spectra correspond to **HSL**<sup>1</sup> free ligand and the corresponding complexes; red line spectra correspond to **HSL**<sup>2</sup> free ligand and the corresponding complexes and blue line spectra correspond to **HSL**<sup>3</sup> free ligand and the corresponding complexes.

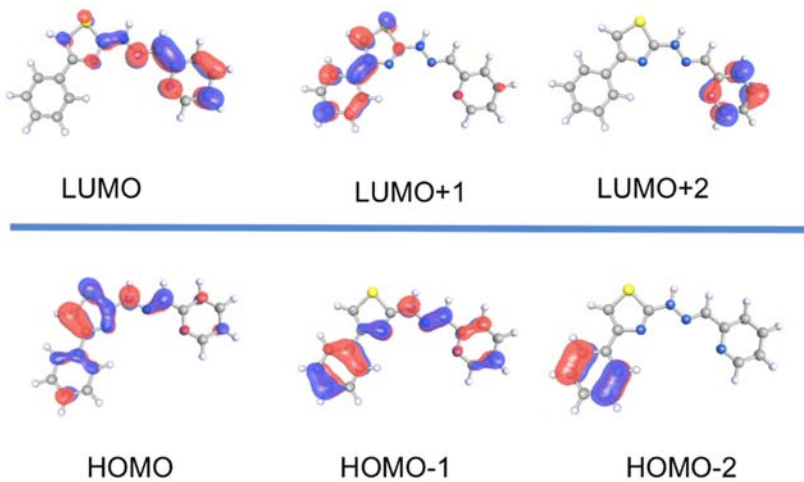


Figure S35. Frontier MOs for optimised **HLS<sup>1</sup>**.

Table S17. TD-DFT singlet-singlet excitation calculations for model system of ligand **HLS<sup>1</sup>**.

model <b>HSL<sup>1</sup></b>			
Transition	$\lambda/\text{nm}$	Oscillator strength	Contributions
$S_0 \rightarrow S_1$	360	0.485	HOMO $\rightarrow$ LUMO
$S_0 \rightarrow S_3$	295	0.137	HOMO $\rightarrow$ LUMO+1
$S_0 \rightarrow S_5$	283	0.470	HOMO-1 $\rightarrow$ LUMO

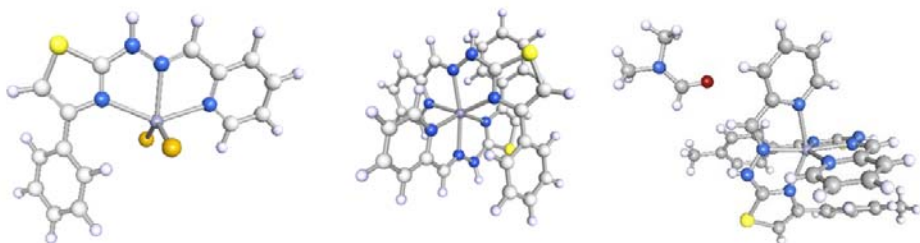


Figure S36. Optimized model systems of **1-Cl** (left), **1-NO<sub>3</sub>** (middle), **3-NO<sub>3</sub>** (right).

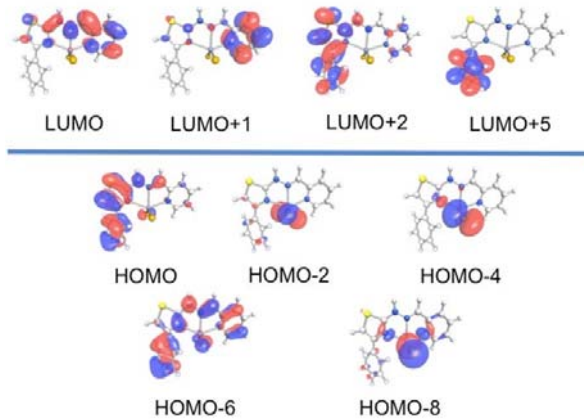


Figure S37. Frontier MOs computed for model system **1-Cl**.

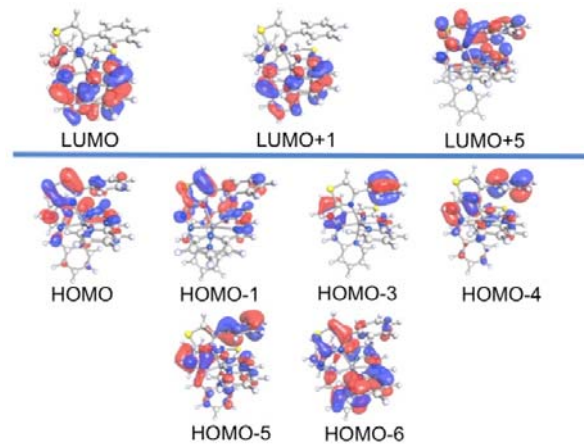


Figure S38. Frontier MOs computed for model system **1-NO<sub>3</sub>**.

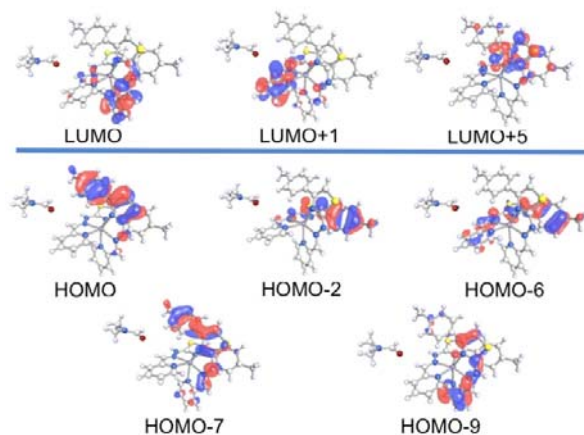


Figure S39. Frontier MOs computed for model system **3-NO<sub>3</sub>**.

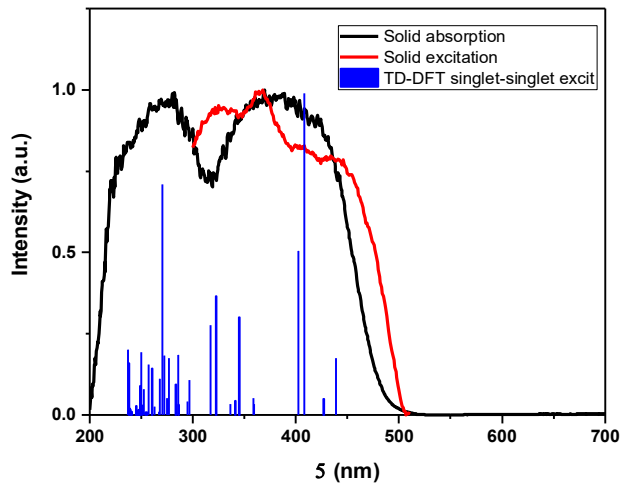


Figure S40. Comparison between experimental absorption and excitation spectra with TD-DFT singlet-singlet excitations for model system **1-Cl**.

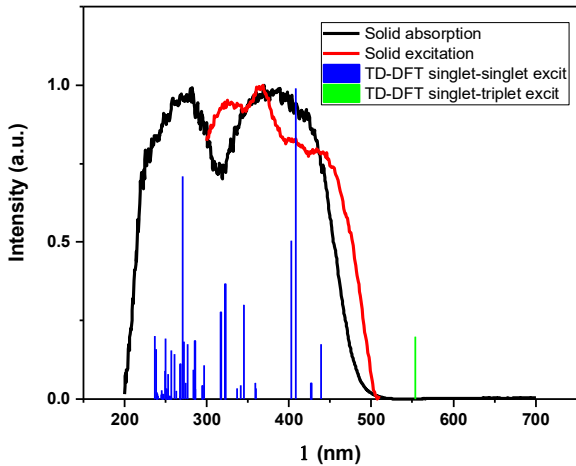


Figure S41. Comparison between experimental absorption and excitation spectra with TD-DFT singlet-singlet and lowest singlet-triplet excitations for model system **1-NO<sub>3</sub>**.

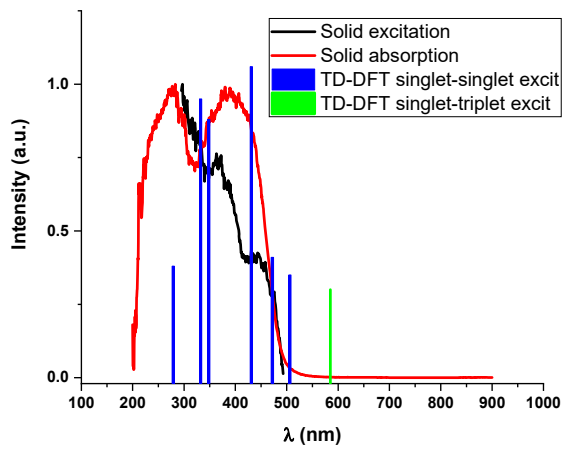


Figure S42. Comparison between experimental absorption and excitation spectra with TD-DFT singlet-singlet and lowest singlet-triplet excitations for model system **3-NO<sub>3</sub>**.

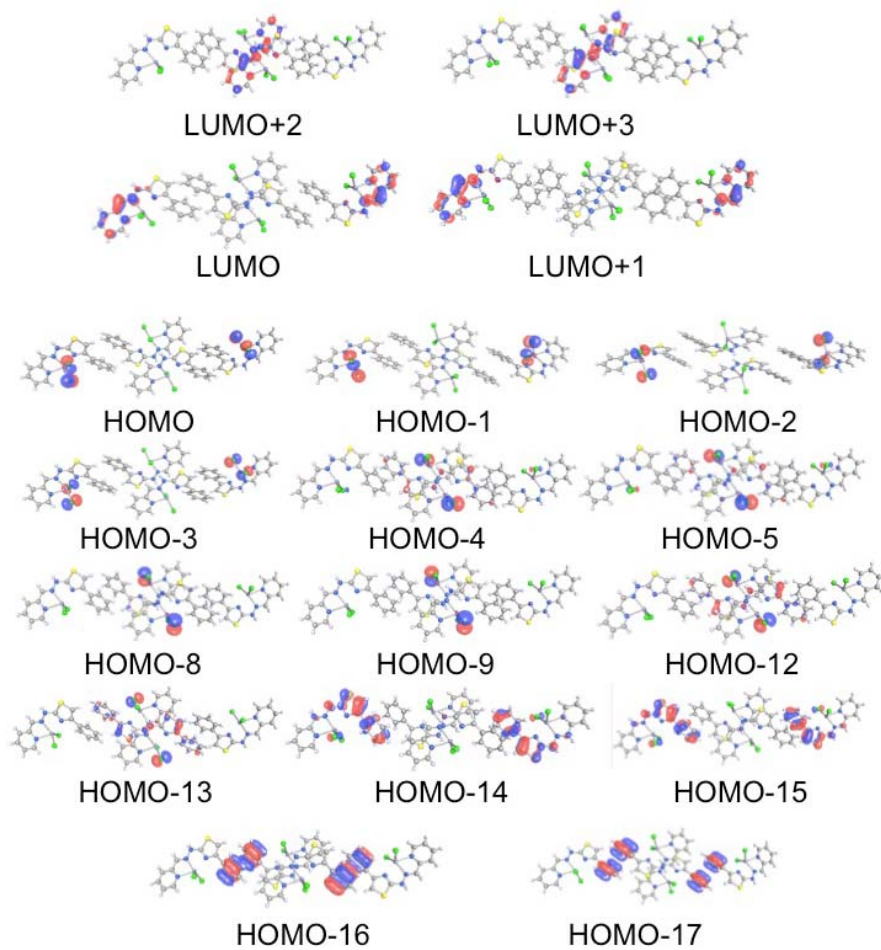


Figure S43. Frontier MOs computed for model system **1-Cl-ext**.

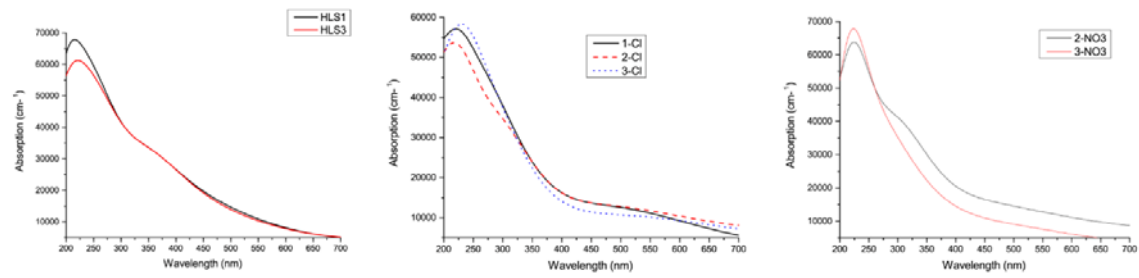


Figure S44. Resulting absorption spectra for **HLS¹** and **HLS³** ligands and complexes **1–3-Cl** and **2–3-NO₃**

XYZ coordinates for optimized model system **1-Cl**

35

C	4.20804	-0.34222	6.51851
H	4.56865	-1.34455	6.71290
C	4.09305	0.56649	7.56003
H	4.34524	0.26370	8.56840
C	3.67549	1.86820	7.30452
H	3.59505	2.58079	8.11567
C	3.37378	2.25404	6.00391
H	3.05362	3.26679	5.79583
C	3.48498	1.34874	4.95904
H	3.23576	1.65597	3.95232
C	3.90299	0.04031	5.20959
C	4.00612	-0.93115	4.11464
C	3.69791	-2.25707	4.20064
H	3.30008	-2.79673	5.04213
C	4.43278	-1.53358	2.02064
C	5.78487	0.07402	-0.79534
H	5.74318	-0.62962	-1.62614
C	6.33661	1.41069	-1.00366
C	6.84470	3.43580	-0.03463
H	6.82970	4.03157	0.86963
C	7.37237	3.92462	-1.22740
H	7.77522	4.92681	-1.27102
C	7.36518	3.10080	-2.34314
H	7.76415	3.44837	-3.28721
C	6.84170	1.81898	-2.23429
H	6.82561	1.14637	-3.08200
N	4.42006	-0.53758	2.85202
N	4.86406	-1.39254	0.71937
N	5.37437	-0.21108	0.37924
N	6.33808	2.21674	0.06690
S	3.94248	-3.05479	2.68184
Cl	3.29377	2.42066	1.42576
Cl	6.88066	1.84224	3.37471
Zn	5.24738	1.43861	1.92838
H	4.76596	-2.14218	0.04809

XYZ coordinates for optimized model system **1-NO<sub>3</sub>**

35

C	4.20804	-0.34222	6.51851
H	4.56865	-1.34455	6.71290
C	4.09305	0.56649	7.56003
H	4.34524	0.26370	8.56840
C	3.67549	1.86820	7.30452
H	3.59505	2.58079	8.11567
C	3.37378	2.25404	6.00391
H	3.05362	3.26679	5.79583
C	3.48498	1.34874	4.95904
H	3.23576	1.65597	3.95232
C	3.90299	0.04031	5.20959
C	4.00612	-0.93115	4.11464
C	3.69791	-2.25707	4.20064
H	3.30008	-2.79673	5.04213
C	4.43278	-1.53358	2.02064
C	5.78487	0.07402	-0.79534
H	5.74318	-0.62962	-1.62614
C	6.33661	1.41069	-1.00366
C	6.84470	3.43580	-0.03463
H	6.82970	4.03157	0.86963
C	7.37237	3.92462	-1.22740
H	7.77522	4.92681	-1.27102
C	7.36518	3.10080	-2.34314
H	7.76415	3.44837	-3.28721
C	6.84170	1.81898	-2.23429
H	6.82561	1.14637	-3.08200
N	4.42006	-0.53758	2.85202
N	4.86406	-1.39254	0.71937
N	5.37437	-0.21108	0.37924
N	6.33808	2.21674	0.06690
S	3.94248	-3.05479	2.68184
Cl	3.29377	2.42066	1.42576
Cl	6.88066	1.84224	3.37471
Zn	5.24738	1.43861	1.92838
H	4.76596	-2.14218	0.04809

XYZ coordinates for optimized model system **3-NO<sub>3</sub>**

83

C	20.982000	27.261000	27.766000
H	21.768000	27.607000	28.197000
H	20.994000	27.503000	26.837000
H	20.967000	26.305000	27.849000
C	19.753000	27.843000	28.422000
C	18.569000	27.982000	27.730000
H	18.520000	27.683000	26.851000
C	17.462000	28.549000	28.306000
H	16.690000	28.661000	27.799000
C	17.472000	28.965000	29.645000
C	18.654000	28.785000	30.354000
H	18.689000	29.028000	31.251000
C	19.776000	28.254000	29.753000
H	20.560000	28.169000	30.245000
C	16.309000	29.560000	30.288000
C	15.000000	29.267000	30.036000
H	14.719000	28.642000	29.407000
C	15.311000	30.924000	31.742000
C	16.390000	33.734000	33.472000
H	15.670000	34.050000	33.968000
C	17.676000	34.446000	33.416000
C	17.859000	35.652000	34.066000
H	17.186000	36.028000	34.585000
C	19.103000	36.286000	33.910000
H	19.257000	37.112000	34.310000
C	20.080000	35.689000	33.176000
H	20.912000	36.093000	33.078000
C	19.814000	34.466000	32.571000
H	20.485000	34.056000	32.074000
N	16.474000	30.527000	31.281000
N	15.210000	31.913000	32.677000
N	16.330000	32.654000	32.795000
N	18.637000	33.860000	32.675000
S	13.934000	30.191000	31.015000
H	14.545000	32.280000	32.808000
C	12.080000	34.160000	29.829000
H	11.678000	33.412000	30.277000
H	11.607000	34.336000	29.012000
H	12.038000	34.933000	30.396000
C	13.531000	33.841000	29.514000
C	14.578000	34.386000	30.233000
H	14.397000	34.991000	30.916000
C	15.882000	34.051000	29.958000
H	16.570000	34.442000	30.446000
C	16.184000	33.138000	28.959000
C	15.133000	32.605000	28.215000

H	15.313000	32.010000	27.523000
C	13.830000	32.950000	28.494000
H	13.141000	32.582000	27.990000
C	17.577000	32.716000	28.685000
C	18.151000	32.610000	27.472000
H	17.724000	32.808000	26.670000
C	19.598000	32.021000	29.304000
C	20.850000	30.882000	32.340000
H	21.748000	30.682000	32.206000
C	20.181000	30.664000	33.618000
C	20.871000	30.246000	34.745000
H	21.790000	30.102000	34.711000
C	20.171000	30.045000	35.923000
H	20.617000	29.771000	36.692000
C	18.816000	30.253000	35.949000
H	18.327000	30.116000	36.728000
C	18.193000	30.674000	34.777000
H	17.274000	30.812000	34.790000
N	18.409000	32.390000	29.747000
N	20.580000	31.623000	30.159000
N	20.113000	31.369000	31.420000
N	18.850000	30.887000	33.641000
S	19.791000	32.060000	27.602000
H	21.104000	31.245000	29.954000
Zn	18.085000	31.892000	31.814000
C	25.215000	26.412000	32.022000
H	25.742000	25.945000	32.675000
H	24.972000	25.807000	31.316000
H	25.725000	27.139000	31.658000
C	23.917000	26.292000	33.881000
H	24.730000	25.829000	34.096000
H	23.742000	26.957000	34.551000
H	23.190000	25.667000	33.852000
C	23.036000	27.613000	32.140000
H	23.107000	27.869000	31.249000
N	24.049000	26.912000	32.631000
O	22.034000	27.952000	32.716000